

UNCLASSIFIED

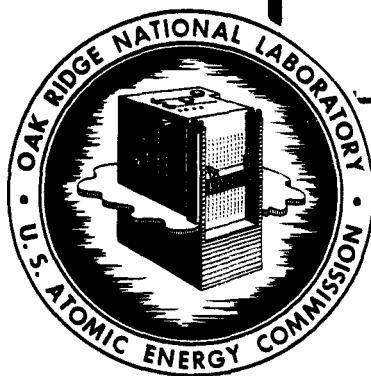


3 4456 0050908 2

ORNL 1005  
Progress Report

*4a*

PHYSICS DIVISION  
QUARTERLY PROGRESS REPORT  
FOR PERIOD ENDING MARCH 20, 1951



OAK RIDGE NATIONAL LABORATORY  
OPERATED BY  
CARBIDE AND CARBON CHEMICALS COMPANY  
A DIVISION OF UNION CARBIDE AND CARBON CORPORATION



POST OFFICE BOX P  
OAK RIDGE, TENNESSEE

UNCLASSIFIED

UNCLASSIFIED

ORNL-1005

This document consists of 63  
pages.

Copy 7 of 229. Series A.

Contract No. W-7405, eng 26

**PHYSICS DIVISION**

A. H. Snell, Director  
E. O. Wollan, Associate Director

**QUARTERLY PROGRESS REPORT**  
**for Period Ending March 20, 1951**

Edited by:  
Seymour Bernstein

DATE ISSUED: JUL 24 1951

**OAK RIDGE NATIONAL LABORATORY**  
operated by  
**CARBIDE AND CARBON CHEMICALS COMPANY**  
A Division of Union Carbide and Carbon Corporation  
Post Office Box P  
Oak Ridge, Tennessee

UNCLASSIFIED



3 4456 0050908 2

## UNCLASSIFIED

ORNL-1005  
Progress Report

## INTERNAL DISTRIBUTION

- |                              |                       |                             |
|------------------------------|-----------------------|-----------------------------|
| 1. G. T. Felbeck (C&CCC)     | 24. J. A. Swartout    | 42. Lewis Nelson            |
| 2-3. Chemistry Library       | 25. A. Hollaender     | 43. R. W. Stoughton         |
| 4. Physics Library           | 26. K. Z. Morgan      | 44. C. E. Winters           |
| 5. Biology Library           | 27. F. L. Steahly     | 45. W. H. Jordan            |
| 6. Health Physics Library    | 28. M. T. Kelley      | 46. E. C. Campbell          |
| 7. Metallurgy Library        | 29. W. H. Pennington  | 47. D. S. Billington        |
| 8-9. Training School Library | 30. E. O. Wollan      | 48. M. A. Bredig            |
| 10-13. Central Files         | 31. D. W. Cardwell    | 49. R. S. Livingston        |
| 14. C. E. Center             | 32. A. S. Householder | 50. C. P. Keim              |
| 15. C. E. Larson             | 33. L. D. Roberts     | 51. J. L. Meem              |
| 16. W. B. Humes (K-25)       | 34. J. A. Lane        | 52. C. E. Clifford          |
| 17. W. D. Lavers (Y-12)      | 35. M. M. Mann        | 53. G. H. Clewett           |
| 18. A. M. Weinberg           | 36. R. N. Lyon        | 54. C. D. Susano            |
| 19. E. H. Taylor             | 37. W. C. Koehler     | 55. C. J. Borkowski         |
| 20. E. D. Shipley            | 38. W. K. Ergen       | 56. M. J. Skinner           |
| 21. E. J. Murphy             | 39. E. P. Blizard     | 57-67. Central Files (O.P.) |
| 22. F. C. VonderLage         | 40. M. E. Rose        |                             |
| 23. A. H. Snell              | 41. G. E. Boyd        |                             |

## EXTERNAL DISTRIBUTION

- 68-79. Argonne National Laboratory
- 80. Armed Forces Special Weapons Project
- 81-86. Atomic Energy Commission, Washington
- 87. Battelle Memorial Institute
- 88. Brush Beryllium Company
- 89-92. Brookhaven National Laboratory
- 93. Bureau of Medicine and Surgery
- 94. Bureau of Ships
- 95-98. Carbide and Carbon Chemicals Company (K-25)
- 99-102. Carbide and Carbon Chemicals Company (Y-12)
- 103. Columbia University (J. R. Dunning)
- 104. Columbia University (G. Failla)
- 105-109. E. I. duPont de Nemours and Company
- 110-113. General Electric, Richland
- 114-117. Idaho Operations Office
- 118-119. Iowa State College
- 120. Kansas City Operations Branch
- 121. Kellex Corporation
- 122-123. Kirtland Air Force Base
- 124-127. Knolls Atomic Power Laboratory
- 128-130. Los Alamos Scientific Laboratory
- 131. Mallinckrodt Chemical Works
- 132. Massachusetts Institute of Technology (A. Gaudin)
- 133. Massachusetts Institute of Technology (A. R. Kaufmann)
- 134-136. Mound Laboratory
- 137. National Advisory Committee for Aeronautics

- 138. National Bureau of Standards (R. D. Huntoon)
- 139. Naval Medical Research Institute
- 140-141. Naval Radiological Defense Laboratory
- 142. New Brunswick Laboratory
- 143-145. New York Operations Office
- 146. North American Aviation, Inc.
- 147. Patent Branch, Washington
- 148. RAND Corporation
- 149. Sandia Corporation
- 150. Santa Fe Operations Office
- 151-165. Technical Information Service, Oak Ridge
- 166-167. U. S. Geological Survey (T. B. Nolan)
- 168-169. U. S. Public Health Service
- 170. University of California at Los Angeles
- 171-175. University of California Radiation Laboratory
- 176-177. University of Rochester
- 178. University of Washington
- 179. Savannah River Operations Office
- 180. Western Reserve University
- 181-184. Westinghouse Electric Corporation
- 185. Yale University
- 186-189. Atomic Energy Project, Chalk River
- 190. Chief of Naval Research
- 191. H. K. Ferguson Company
- 192. Harshaw Chemical Company
- 193. Isotopes Division (Mr. McCormick)
- 194-195. Library of Congress, Acquisition Department (J. W. Cormn)
- 196. National Bureau of Standards
- 197. National Research Council, Ottawa
- 198. Naval Research Laboratory
- 199-200. Nevis Cyclotron Laboratories
- 201-202. Oak Ridge Institute of Nuclear Studies
- 203-212. United Kingdom Scientific Mission (M. Greenhill)
- 213. USAF, Eglin Air Force Base (Technical Library)
- 214. USAF, Wright-Patterson Air Force Base (Rodney Nudenberg)
- 215-219. USAF, Wright-Patterson Air Force Base (CADO)
- 220. U. S. Army, Army Field Forces (Captain James Kerr)
- 221. U. S. Army, Atomic Energy Branch (Lt. Col. A. W. Betts)
- 222. U. S. Army, Director of Operations Research (Dr. Ellis Johnson)
- 223. U. S. Army, Office, Chief of Ordnance (Col. A. R. Del Campo)
- 224-225. U. S. Army, Office of the Chief Signal Officer (Curtis T. Clayton  
thru Major George C. Hunt)
- 226-228. U. S. Army, Technical Command (Col. J. H. Rothschild  
Attn: Technical Library)
- 229. UT-AEC Agricultural Research Program (Charles S. Hobbs)

UNCLASSIFIED

Physics Division quarterly progress reports previously issued in this series are as follows:

ORNL-325 Supplement	December, January, and February, 1948-49
ORNL-366	Period Ending June 15, 1949
ORNL-481	Period Ending September 25, 1949
ORNL-577	Period Ending December 15, 1949
ORNL-694	Period Ending March 15, 1950
ORNL-782	Period Ending June 15, 1950
ORNL-865	Period Ending September 20, 1950
ORNL-940	Period Ending December 20, 1950

UNCLASSIFIED

TABLE OF CONTENTS

INTRODUCTION AND SUMMARY	7
PUBLICATIONS	12
1. NEUTRON DIFFRACTION	13
Metal Hydrides	13
Scattering Cross-Sections	13
Magnetic Structure of $MnF_2$ and $NiF_2$	14
2. NEUTRON-DECAY EXPERIMENT	18
3. NUCLEAR-ALIGNMENT PROGRAM	20
Measurement of Temperature	20
Measurement of Entropy of Magnetization	21
4. SHORT-LIVED ISOMERS	24
5. HIGH-VOLTAGE PROGRAM	25
Scintillation-Counter Gamma-Ray Spectra	26
Reactions with $He^3$	26
Inelastic Scattering of Neutrons	31
6. STANDARD REACTOR	36
7. HEAVY-ION RESEARCH	37
8. NEUTRON-SENSITIVE PHOSPHORS	38
9. SHORT-PERIOD ACTIVITIES	42
Pulse Analyses by Photographic Densities	42
Fermi Plots of $Ag^{110}$ (24-sec) and $Ag^{108}$ (2.4-min) Beta Spectra	46
10. LONG-WAVELENGTH NEUTRONS	49
11. THEORETICAL PHYSICS	50
Angular Correlation of Internal-Conversion Electrons and Gammas	51
Angular Correlation of Three Successive Radiations	51
Polarization Effects in Neutron Capture	51
Hyperfine Structure in $Mn^{++}$	52
On the Energy-Loss Mechanism of Slow Ions	54
Neutron-Deuteron Scattering	55
Theory of Scattering and Capture of Slow Neutrons	58
A Note on Isotropy of Nuclear Gamma Radiation	62
Symmetry Between Positron and Negatron Spectra in Beta Decay	63

## UNCLASSIFIED

## LIST OF FIGURES

Fig. 1	Typical Diffraction Patterns for $\text{MnF}_2$ at 300°K and 24°K	15
Fig. 2	Magnetic Structure of $\text{MnF}_2$	17
Fig. 3	Effect of Neutron Flipper; Intensity of Second Crystal as a Function of Alternating Magnetic Field Strength	23
Fig. 4	Simultaneous Yields of 12- and 16-Mev Gamma Ray of $\text{B}^{11} + \text{H}^1 \longrightarrow \text{C}^{12} + \gamma$	27
Fig. 5	Gamma Ray Spectrum of $\text{B}^{11} + \text{H}^1 \longrightarrow \text{C}^{12} + \gamma$	28
Fig. 6	Differential Pulse Height Spectrum of $\text{H}^2 + \text{H}^1 \longrightarrow \text{He}^3 + \gamma$	29
Fig. 7	Differential Pulse Height Spectrum of $\text{H}^3 + \text{H}^1 \longrightarrow \text{He}^4 + \gamma$	30
Fig. 8	Thick Target Yield of Protons from $\text{He}^3 + \text{H}^2 \longrightarrow \text{He}^4 + \text{H}^1 + 18.6 \text{ Mev}$	32
Fig. 9	Angular Distribution of Protons from $\text{He}^3 + \text{H}^2 \longrightarrow \text{He}^4 + \text{H}^1 + 18.6 \text{ Mev}$	32
Fig. 10	Geometry for Inelastic Neutron Scattering Experiment	33
Fig. 11	Histogram of Inelastic Scattering in Lead	35
Fig. 12	X Rays from $\text{Cd}^{109}$ (330 d) as Detected by Krypton-Methane Filled Proportional Counter	43
Fig. 13	X Rays from $\text{Eu}^{152}$ (9.2 hr) as Detected by Xenon-Methane Filled Proportional Counter	45
Fig. 14	Fermi Plot of $\beta$ -Spectrum of 2.4-min $\text{Ag}^{108}$	47
Fig. 15	Fermi Plot of $\beta$ -Spectrum of 24-sec $\text{Ag}^{110}$	48

## INTRODUCTION AND SUMMARY

This report covers unclassified work of the Physics Division for the period December 20, 1950 to March 20, 1950. The classified section of the Physics Division quarterly report appears separately (ORNL-1006).

The additions to the research staff in the Physics Division are: Mr. C. F. Barnett (Heavy Ion Research Group) and Mrs. Mary P. Haydn (Shielding Group). Mr. Barnett was formerly with the Cyclotron Group at Y-12. Mrs. Haydn was formerly with the United States Bureau of Mines at Norris.

### Neutron Diffraction

Preliminary studies of the hydrides of titanium and cerium have been made. Further investigation is required before definite hydrogen positions can be established, but it seems certain that a definite structure is present. The coherent scattering cross-section of cerium was found to be 2.2 barns, positive phase; that of barium, 3.5 barns, positive phase.

The magnetic structure of  $MnF_2$  and  $NiF_2$  have been studied. The diffraction patterns show that for both these compounds there is an ordering of the atomic magnetic moments below  $70^\circ K$ . A model of the magnetic structure consistent with the data is given. The diffraction results are compared with those from susceptibility measurements.

### Neutron-Decay Experiment

Changes in the geometry of the apparatus with respect to the neutron beam have resulted in a much clearer revelation of the neutron-decay effect. There are now about 1.5 beta-proton coincidences per minute which stand out well above the background rate. Attention is being focused upon those factors involved in a more accurate determination of the lifetime; the beta counter efficiencies are being measured; the volume in which neutron decays are being observed is being more clearly defined by means of potential barriers.

## Nuclear-Alignment Program

In connection with the nuclear-alignment program, a new method for the measurement of absolute temperature and entropy below 1°K is being developed.

The "molecular" beam magnetic resonance method has been adapted for use in the nuclear-alignment program. By its use, the aligned nuclei-polarized neutron interaction can be studied with parallel or antiparallel orientations without changing any of the large magnetic fields involved in the neutron and nuclear alignment. The method has been found to be very convenient, also, in studying polarization and depolarization of neutrons.

## Short-lived Isomers

An excited state in  ${}_{66}\text{Dy}^{160}$  with a half-life of  $1.8 \times 10^{-9}$  sec has been observed with the delayed-coincidence scintillation spectrometer using sources of  $\text{Tb}^{160}$ .

## High-Voltage Program

The angular distribution of the gamma rays from the reaction  $\text{B}^{11}(p,\gamma)\text{C}^{12}$  are being studied. The 12-Mev gamma ray was reported to be emitted anisotropically with respect to the beam. The anisotropy of the 16-Mev gamma ray has been found to be, at most, several percent. The available evidence indicates that if these two gamma rays start from different initial levels, these levels are less than 1 Kev apart.

The gamma rays from the capture of protons by  $\text{H}^2$  and  $\text{H}^3$  are being studied with the scintillation spectrometer. Preliminary results are given.

Apparatus has been constructed to make possible the routine acceleration of  $\text{He}^3$ . The reaction,  $\text{He}^3 + \text{H}^2 \longrightarrow \text{He}^4 + \text{H}^1$  is being studied and is to be compared with  $\text{H}^3 + \text{H}^2 \longrightarrow \text{He}^4 + n$ .

A preliminary experiment on the inelastic scattering of 14-Mev neutrons by lead has been carried out. A histogram of the energy spectrum of the scattered neutrons is shown.

### **Standard Pile**

The Laboratory standard graphite pile is being recalibrated in order to clear up existing discrepancies between Argonne measurements and those of Haydn Jones of several years ago at ORNL. The neutron source being used in the standard pile work was compared by the Bureau of Standards to one of their sources. Apparatus is being set up for making an independent determination of the absolute number of neutrons being emitted by our source.

### **Heavy-Ion Research**

Work on the behavior of thin evaporated films upon bombardment with 200-Kev protons has been initiated. The films were first made radioactive by neutron capture so that the effect of the proton bombardment could be studied using the spatial distribution of the radioactivity before and after bombardment. Studies of various types of heavy-ion detectors and of ion sources are being continued.

### **Neutron-Sensitive Phosphors**

A number of neutron-sensitive phosphors containing lithium have been prepared in microcrystalline form, and their luminescent properties have been observed. Some of these have been found to have a decay time short enough to be of interest. Apparatus has been constructed to determine the crystal-growth properties of phosphors and to grow large crystals from the melt in a controlled atmosphere.

### **Short-Period Activities**

The use of a photographic-density technique in studying short-period activities has been described in previous quarterly reports (see p. 3 for ORNL numbers). The results obtained from this technique of pulse-height analysis have now been compared to the results obtained from the conventional type of pulse-height analyzer. Data are given which show that the two techniques give comparable results. The density method has the advantage of being less laborious and better adapted for short periods.

The data on the beta spectra of  $\text{Ag}^{108}$  and  $\text{Ag}^{110}$  described in the last quarterly report (ORNL-940, p. 19) have been examined further. Fermi plots and beta-ray-energy end points resulting from this more exact analysis are given in this report.

### Long-Wavelength Neutron Source

A source of low-energy neutrons of wavelength greater than 4 Å is being developed. It makes use of the critical-angle property of total reflection to eliminate higher order Bragg reflections from a crystal.

### Theoretical Physics

A list of problems in which the Theoretical Physics Group is currently interested is given in this report (p. 50), together with an indication of the status of each.

The problem of the angular correlation of internal-conversion electrons and gamma rays in a cascade transition has been set up for computation.

The general problem of determining the coincidence counting rates in a nuclear cascade process for three radiations emitted (or absorbed) at arbitrary angles has been solved. A detailed report giving proofs and applications to  $\text{B}^{11}(p, \gamma\gamma)\text{C}^{12}$  is being prepared.

The problem of the polarization of the gamma rays resulting from capture of polarized neutrons as a function of angle has been studied. For both pure and mixed multipoles the radiation is isotropic and does not depend on the neutron polarization. A report of the work is being prepared.

Calculations are in progress to check the hyperfine structure pattern observed by the magnetic resonance method in manganese ammonium sulfate. This effort is in cooperation with the experimental nuclear-alignment program.

Investigations of the energy losses of ions in passing through matter are continuing. The calculation of the elastic scattering cross-sections in the low-energy region are well underway. An attempt is being made to formulate a semiempirical theory in the region of ion velocities about equal to orbital electron velocities.

An attempt is being made to use the available information on the  $H^3$  binding energy and the low-energy neutron-deuteron scattering to obtain new information about nuclear forces. By combining these two types of data, a unique choice is described in this report between the two possible pairs of scattering amplitudes for the doublet and quartet states derived from the slow-neutron scattering data.

A simple derivation has been attempted of the usual Breit-Wigner one-level formula. The resulting expression leads to the same shape near resonance, but discrepancies appear for energies more than one-half-width away from resonance.

It has been shown that if one has isotropic  $2^L$  pole gamma radiation from a level of quantum number  $j$ , then a necessary and sufficient condition for all gamma radiation from that state to be isotropic is that  $L \geq j - \frac{1}{2}$ .

## PUBLICATIONS

The following articles by members of the Physics Division have appeared during the past quarter:

1. *Transport Parameters for Thermal Neutrons in Water*, Francis J. Sisk, ORNL-933 (Mar. 15, 1951).
2. "Elementary Pile Theory," H. Soodak and E. C. Campbell, translation into the Russian, *Uspekhi Fiz. Nauk* **42**, 93 (1950).
3. "Neutron Decay: The Problem and the Experiments," Arthur H. Snell, *Nucleonics*, p. 3, March, 1951 .
4. "New Experimental Method for Measuring Absolute Temperatures," L. D. Roberts and J. W. T. Dabbs, *Natl. Bur. Stand. Low-Temperature Symposium*, March 27-29, 1951.
5. "Isotopes Shifts in the Balmer Spectrum of Tritium," H. Pomerance and D. Terranova, *Am. J. Phys.* **18**, 466 (1950).

## 1. NEUTRON DIFFRACTION

C. G. Shull            E. O. Wollan  
                          W. C. Koehler

**Metal Hydrides.** Neutron-diffraction studies of the hydrides of titanium and cerium have been undertaken in an effort to discover if the hydrogen atoms go into definite lattice positions in these substances. The titanium hydride study was made at the request of Dr. B. Matthias of the University of Chicago, and the sample used in the study was a product of Metal Hydrides, Inc. The X-ray diffraction pattern of this sample could be indexed on a face-centered cubic lattice of lattice period  $a_1 = 4.40$  A. No additional lines appeared in the neutron pattern, and the relative intensities suggest that the hydrogen atoms enter the lattice in the sites corresponding to those of fluorine in the  $\text{CaF}_2$  structure. Assuming that the  $\text{CaF}_2$  structure is a correct model, the absolute intensities suggest a composition in this preparation corresponding to  $\text{TiH}_{1.25}$ . Needless to say, further investigation is required before definite hydrogen positions can be established, but it does seem certain that hydrogen forms a definite structural entity with titanium.

A sample of  $\text{CeH}_2$  was submitted by Dr. J. Singer of Los Alamos Scientific Laboratory. The analysis of the data is not yet complete, but it is certain that a definite compound has been formed. A complete report on this work will probably be issued from Los Alamos.

**Scattering Cross-Sections.** In the course of investigating the structure of  $\text{CeH}_2$ , it was necessary to determine the scattering cross-section and phase of cerium. A sample of  $\text{CeO}_2$  was prepared from c.p. cerium nitrate by precipitation of the hydroxide and subsequent ignition. X-ray-diffraction patterns established the formation of  $\text{CeO}_2$ . From the analysis of the neutron-diffraction pattern of  $\text{CeO}_2$ , the coherent scattering cross-section of cerium was found to be 2.2 barns and the phase of scattering was found to be positive. This value of 2.2 barns is much smaller than the potential scattering cross-section of cerium. Since the two major isotopes of cerium are even-even nuclei, it appears that the scattering properties of one or both of these isotopes are strongly influenced by resonances. A study of isotopically enriched samples is planned for the near future.

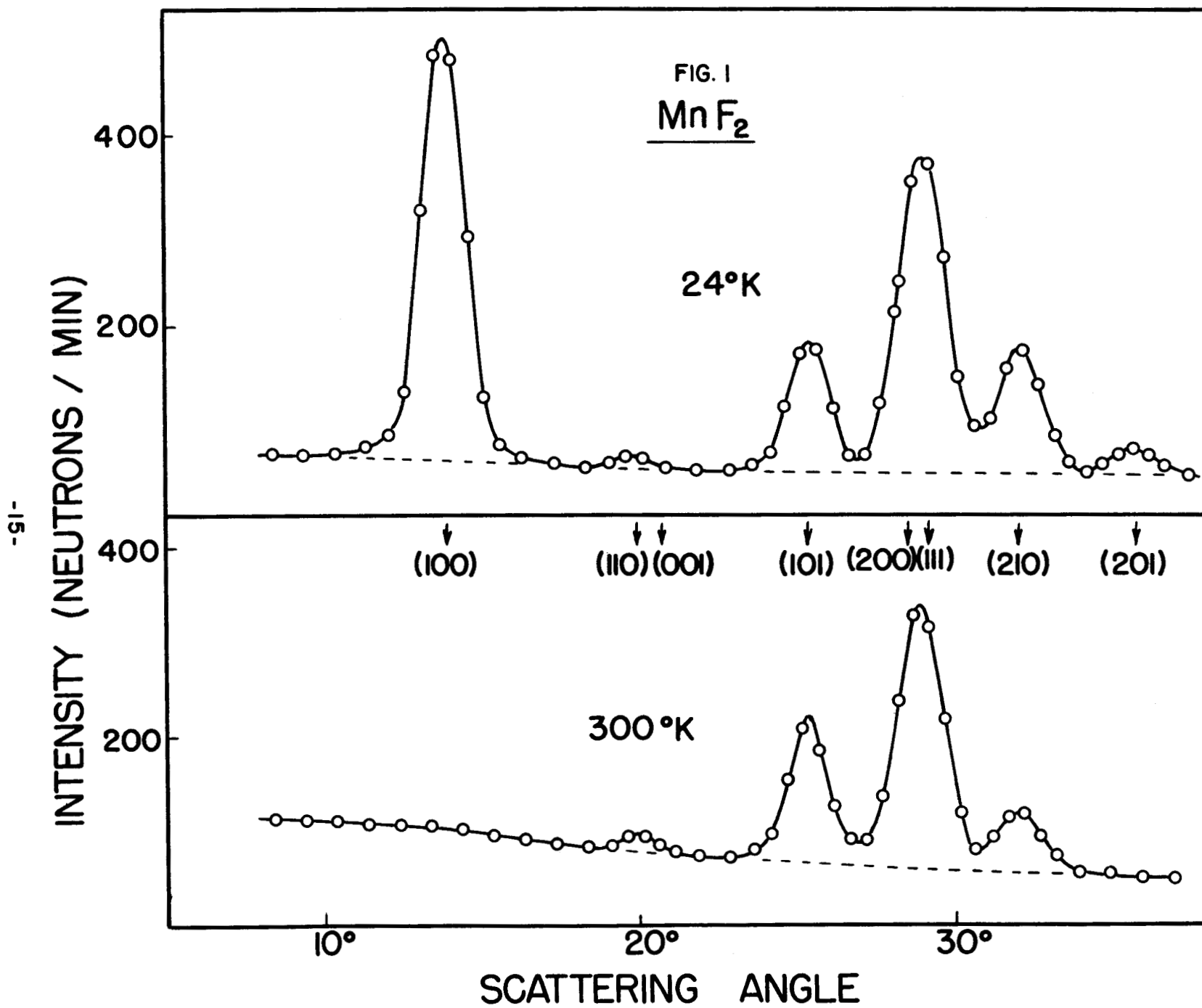
The cross-section of barium was evaluated from the neutron-diffraction pattern of  $\text{BaF}_2$  with the result that  $\sigma_{\text{Ba}} = 3.5$  barns. Barium also scatters with positive phase. Here, also, the small observed cross-section would indicate the presence of resonance effects in one or more of the isotopes.

**Magnetic Structure of  $\text{MnF}_2$  and  $\text{NiF}_2$**  (R. A. Erickson,\* ORINS Fellow). Neutron diffraction studies of  $\text{MnF}_2$  and  $\text{NiF}_2$  have been made at several temperatures between 10 and 300°K. The powdered samples were contained in an evacuated cryostat which utilized a thermal shield cooled by liquid nitrogen to reduce the heat transfer to the working coolant. The coolants employed were pumped liquid or solid nitrogen for temperatures between 45 and 80°K and liquid hydrogen or helium for temperatures below 25°K. The heat leak to the inner coolant was approximately 100 cal/hr and the capacity of the container was sufficient to give about 12 hr of operation from one filling of liquid helium.

The antiferromagnetism of  $\text{MnF}_2$  below 72°K has been established by the powder susceptibility measurements of Bizette and Tsai,<sup>(1)</sup> and the specific heat determination by Stout and Adams.<sup>(2)</sup> From susceptibility measurements on a single crystal of  $\text{MnF}_2$ , Griffel and Stout<sup>(3)</sup> have shown that in the antiferromagnetic state the magnetic moments of the manganese ions are directed along the short axis of the tetragonal system. The powder susceptibility of  $\text{NiF}_2$  has been studied by De Haas, Schultz, and Koolhaas<sup>(4)</sup> and by Bizette<sup>(5)</sup> and from these data no evidence of antiferromagnetism in  $\text{NiF}_2$  was found.

Neutron-diffraction patterns show that for both these compounds there is an ordering of the atomic magnetic moments at temperatures below 70°K. This ordering is evidenced by a progressive decrease in the magnetic diffuse scattering as the temperature is decreased (below 70°K) and the simultaneous growth of superlattice diffraction peaks. At the lowest temperatures the intensity of the magnetic reflections approaches saturation. Typical diffraction patterns for  $\text{MnF}_2$  at 300°K and at 24°K are shown in Fig. 1. The  $\text{NiF}_2$  patterns were entirely analogous to those of  $\text{MnF}_2$ , showing that a magnetic structure similar to that of  $\text{MnF}_2$  has developed at low temperatures.

- (1) Bizette, H., and Tsai, B., "Magnetic Susceptibility of Manganous Fluoride to Low Temperature," *Compt. rend.* 209, 205 (1939).
- (2) Stout, J. W., and Adams, H. E., "Magnetism and the Third Law of Thermodynamics. The Heat Capacity of Manganous Fluoride from 13 to 320°K," *J. Am. Chem. Soc.* 64, 1535 (1942).
- (3) Griffel, M., and Stout, J. W., "The Magnetic Anisotropy of Manganous Fluoride Between 12 and 295°K," *J. Chem. Phys.* 18, 1455 (1950).
- (4) De Haas, W. J., Schultz, B. H., and Koolhaas, J., "Further Measurements of the Magnetic Properties of Some Salts of the Iron Group at Low Temperatures," *Physica* 7, 57 (1940).
- (5) Bizette, H., "On the Orientation of Some Molecules and Crystals by the Magnetic Field. I. Magneto- and Electro-optic Properties of Nitric Oxide," *Ann. phys. Paris* 1, 295-334 (1946).



UNCLASSIFIED  
DWG. 11469

Since the magnetic reflections [in Fig. 1 these are the (100), (201), and parts of the (111) and (210)] can be indexed from the same cell as the nuclear peaks, it follows that the magnetic unit cell is the same size as the chemical unit cell. From the absolute intensity of the magnetic peaks near saturation [particularly from the (100) and the absence of the (001) reflection], the conclusion of Griffel and Stout<sup>(3)</sup> has been verified. A model of the magnetic structure consistent with these data is shown in Fig. 2, where the arrows indicate the direction of the magnetic moment vector.

UNCLASSIFIED  
DWG. 11470

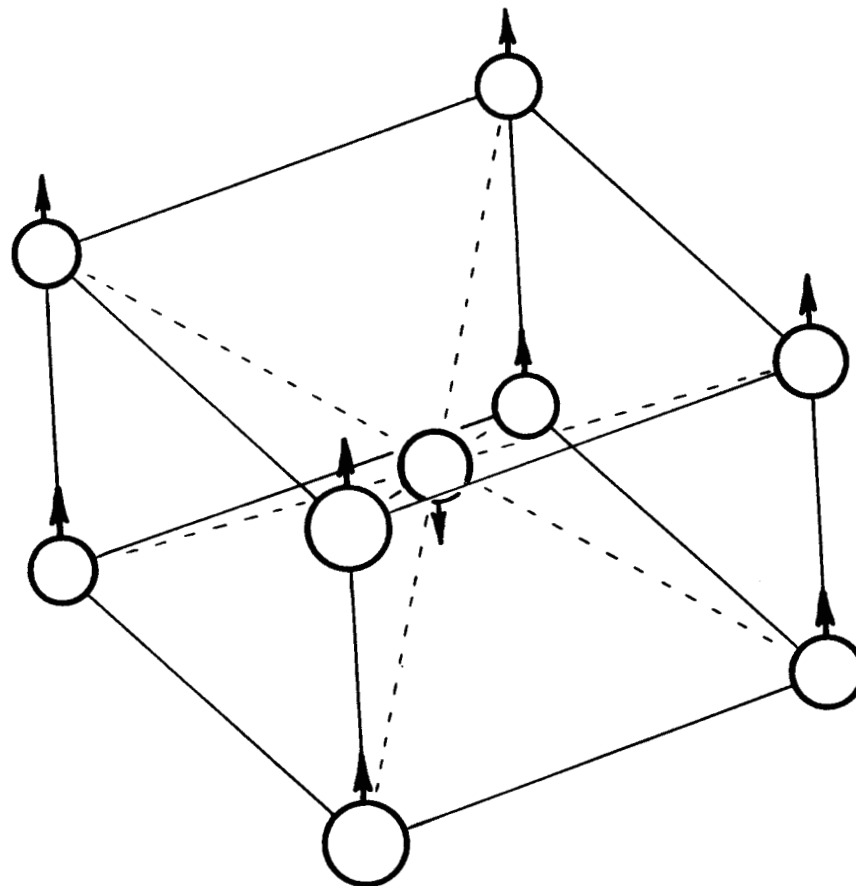


FIG. 2

MAGNETIC STRUCTURE OF MnF<sub>2</sub>

## 2. NEUTRON-DECAY EXPERIMENT

F. Pleasonton            R. V. McCord\*  
A. H. Snell

Since our last report (ORNL-694) the following changes and improvements have been made in the apparatus:

1. The old collimator, which initially delivered a 3-in.-diameter beam subsequently throttled down to  $1\frac{1}{2}$  in., was replaced by a new one which leaked much less around the periphery. The beam at its narrowest is now  $\frac{3}{4}$  in. in diameter but is about  $1\frac{3}{8}$  in. in diameter at the position of the detectors.
2. This change permitted moving the beta counters (of which there are now three) much closer to the beam, and the background was so reduced that the B counters could be abandoned. (The beta counters were two-celled, the cell near the beam being designated A, and that remote from the beam being designated B.) The net change is a great improvement in the geometrical arrangement for coincidence counting.
3. This improvement in geometry has resulted in a much clearer revelation of the neutron-decay effect. We now have about 1.5 beta-proton coincidences per minute, and these counts stand well above the random rate.
4. One of the main obstacles in the evaluation of an accurate half-life had been the exact delineation of the volume of beam from which coincidences were detectable. We believe that this difficulty has been dissolved by the use of potential barriers at either end of the collecting volume, where insulated aluminum rings have been placed around the beam and kept at a potential considerably more positive than their surroundings. The result is that no protons recoiling from neutron decay can pass in or out of the ends of the collecting volume. We believe from rubber sheet tests that essentially all protons created in the volume will be accelerated out toward the multiplier. If successful, this modification will dispose of the main uncertainty in the neutron half-life determination. The potential barriers have been observed to increase the coincidence rate roughly by the amount expected.

The developments outlined above leave the beta-counter efficiency as the main datum yet to be determined for the half-life measurement. Attempts to obtain this quantity have been made by (1) purely geometric considerations,

\*Now with Operations Division.

and (2) use of a calibrated  $\text{Tl}^{204}$  source with the counters in air. The results were so discrepant that we have chosen a third line of attack and are at present making the measurement by the beta-gamma coincidence method. A sodium iodide—crystal scintillation counter has been set up, and beta-gamma coincidences of  $\text{Au}^{198}$  have been observed. The measurement will proceed when the shop delivers the positioning mechanism which will support the source in the actual evacuated tank that is used in the neutron-decay work.

### 3. NUCLEAR-ALIGNMENT PROGRAM

L. D. Roberts                      C. P. Stanford  
J. W. T. Dabbs                     T. Stephenson  
S. Bernstein

In connection with the nuclear-alignment program, a new method for the measurement of absolute temperature and entropy below 1°K is being developed. This method is based on integrals proposed by Casimir,

$$\Delta S = \int (\partial M / \partial T)_H dH$$

with temperature constant, and

$$\Delta T = \int (\partial M / \partial S)_H dH$$

with entropy constant. Our method may be used to measure either of these integrals. The experimental method is discussed below.

**Measurement of Temperature.** Two identical secondary coils, connected in opposition, are placed in the highly uniform field of a large solenoid magnet. In each of these coils a sphere of paramagnetic salt is placed and their positions are so adjusted that the net quantity of charge generated in the secondary circuit, upon switching off a field  $H$  from the large solenoid, will be proportional to the difference of magnetic moment of the two spheres,  $\Delta M(H)$ . When this adjustment has been made, an adiabatic demagnetization of the two spheres is performed as follows: With the help of an auxiliary coil, the two spheres are now isothermally magnetized to slightly different fields, and thus to slightly different entropies at 1°K. The system is now made adiabatic and the demagnetization is performed. In this demagnetization the above known entropy difference,  $\Delta S_0$ , will be essentially constant. Then,  $\Delta M(H)$  is measured isentropically as a function of  $H$  as indicated above for this  $\Delta S_0$ . The required partial derivative is then  $\Delta M(H) / \Delta S_0$ , and the temperature interval  $\Delta T(H)$  may be obtained by the graphical integration of this quantity.

**Measurement of Entropy of Magnetization.** For this measurement the two salt samples are placed in separate liquid helium baths. With these baths at the same temperature, the apparatus is balanced as before so that the signal from the two secondary coils containing the two spheres of salt will be proportional to the difference of magnetic moment,  $\Delta M(H)$ . Then the two baths are pumped to two slightly different temperatures, differing by an increment  $\Delta T$ , and  $\Delta M(H)$  is measured isothermally as a function of  $H$  for this  $\Delta T$ . The required partial derivative is now  $\Delta M(H)/\Delta T$  and the entropy interval  $\Delta S(H)$  is obtained by graphical integration as before.

The equipment for these experiments has just been completed and preliminary experiments are being performed.

In January three of the eight coils of the large electromagnet used for the nuclear-alignment work were burned out. This event hampered the alignment program considerably as it took some time to make even a temporary repair of the magnet. By reshaping and enlarging the pole pieces, according to a prescription of Dwight and Abt,<sup>(1)</sup> the efficiency of the magnetic circuit was somewhat improved so that we now have approximately the same fields with five coils that we previously had with eight. During this period the low-temperature nuclear-alignment equipment has also been revised for greater convenience of operation, and apparatus for temperature measurement below  $1^\circ\text{K}$  has been installed. The equipment is in satisfactory operation. In a test run, a sample of manganous ammonium sulfate was demagnetized to a field of 400 gauss, and the Curie temperature  $T^*$  was measured as a function of time. The temperature remained very constant at about  $0.1^\circ\text{K}$ , the variation being immeasurably small for more than 3 hr.

Use of a neutron flipper can nearly double the effect due to nuclear alignment. This was discussed in the last quarterly report (ORNL-940, p. 12). The beam reflected from a magnetized magnetite crystal is excellent for investigating the operation of a neutron flipper.

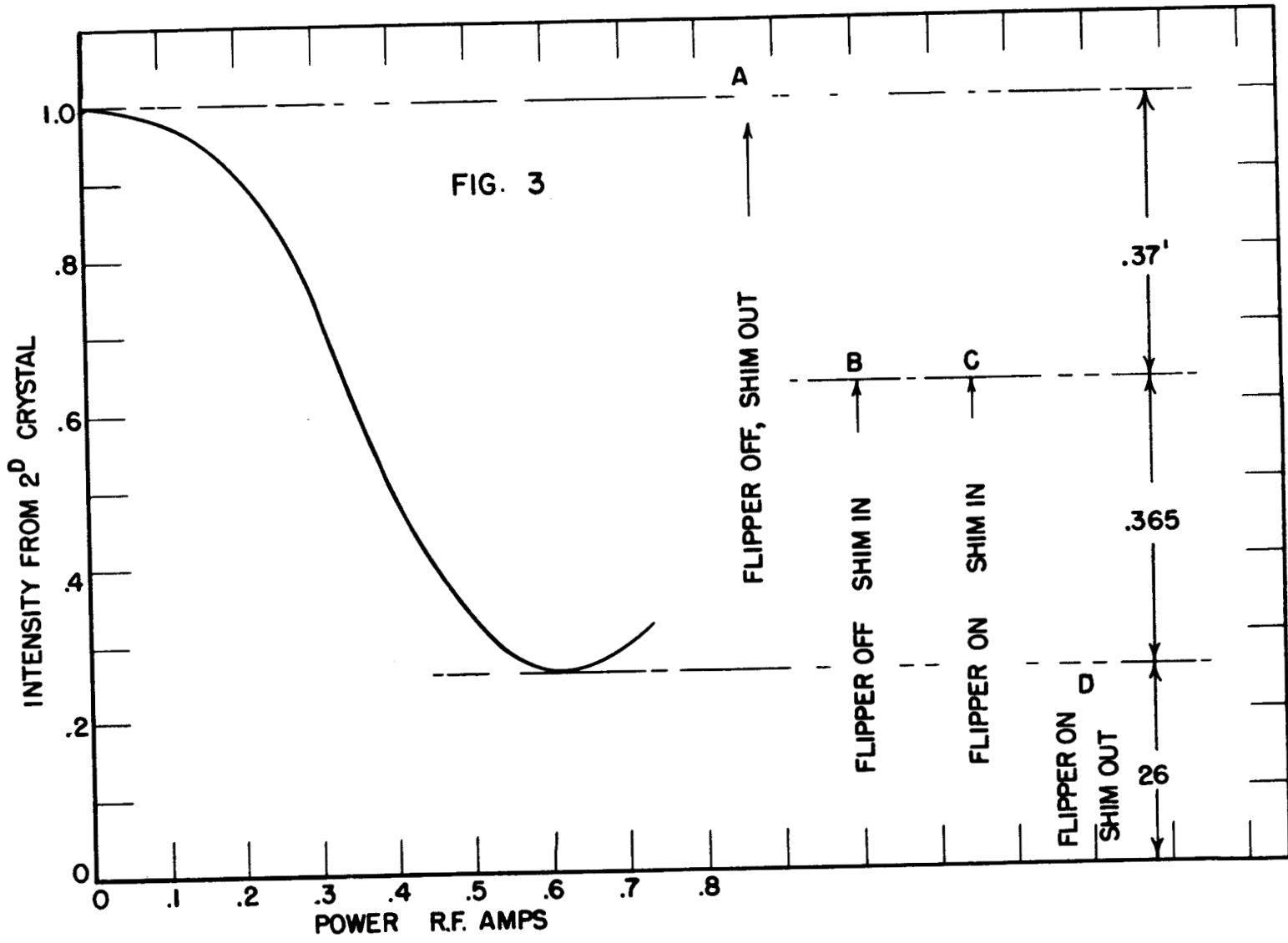
A magnetite crystal was used as a monochromator and polarizer, and a second magnetite crystal was used as a beam analyzer. The neutron-flipping coil was placed between the two crystals. If the reflected beam from the

(1) Dwight, H. B., and Abt, C. F., "The Shape of Core for Laboratory Electromagnets," *Rev. Sci. Instruments* 7, 144 (1936).

crystal was 100% polarized and the flipper 100% efficient, then the intensity from the second crystal would go to zero when the flipper was turned on. Figure 3 shows the intensity from the second crystal as a function of the strength of the alternating magnetic field. The intensity drops to about 26% for optimum power and frequency. To find whether the lack of polarization from the first crystal or the flipper efficiency was responsible for the remaining 26%, a depolarizing iron shim was used. The extent of the depolarization by the iron shim may be checked using the neutron flipper. The figure shows that the intensity is unchanged by turning on the flipper when the shim is between polarizer and analyzer. Therefore, the shim completely depolarizes the beam.

Next, by comparing the intensity difference between no shim or flipper and shim only (*AB*) with the intensity difference between shim only and flipper only (*BD*) we find the flipper is about 100% efficient for monoenergetic neutrons and that the beam from the first crystal is about 80% polarized.

Using the same method with a heterogeneous beam of neutrons (polarized by transmission through 4 cm of iron), we find the flipper to be about 80% efficient.



#### 4. SHORT-LIVED ISOMERS

F. K. McGowan

An excited state in  ${}_{66}\text{Dy}^{160}$  with a half-life of  $(1.8 \pm 0.2) \times 10^{-9}$  sec has been observed with the delayed-coincidence scintillation spectrometer using sources of  $\text{Tb}^{160}$ .

The beta spectrum of  $\text{Tb}^{160}$  is known to consist of at least two components, of 860 and 521 Kev maximum energy, respectively, accompanied by a rather large number of conversion lines corresponding to gamma rays with energies 85, 198, 300, 886, and 965 Kev.<sup>(1)</sup>

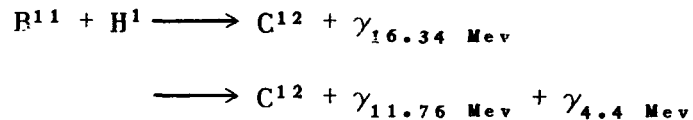
Preliminary measurements of the radiation announcing the formation of the metastable state indicate that the metastable state follows at least the higher energy component of the beta spectrum. The radiation from the decay of the metastable state appears to be only the 85-Kev gamma-ray transition.

(1) Burson, S. B., Blair, K. W., and Saxon, D., "Beta-Spectrum and Decay Scheme of  ${}_{65}\text{Tb}^{160}$ ," *Phys. Rev.* 77, 403.

## 5. HIGH-VOLTAGE PROGRAM

C. D. Moak and G. Robinson

The study of the gamma rays from the reaction



has continued with two ends in view: (1) to eventually make an assignment of angular momenta and parity on the levels in  $\text{C}^{12}$  giving rise to the gamma rays, and (2) to utilize the gamma rays, whose energies have been measured,<sup>(1)</sup> for calibrating the scintillation gamma-ray spectrometer. The spectrum study is discussed in this section.

It was reported in the last quarterly report (ORNL-940, p. 40) that the 12-Mev gamma ray shows an angular distribution with the beam of the form  $A + B \cos^2 \theta$  with  $B/A = 0.15 \pm 0.03$ . Since the 12-Mev gamma ray is emitted first,<sup>(1)</sup> it is of interest to compare the angular distribution of the 16-Mev gamma ray, which is emitted in competition with the 12-Mev gamma ray. Earlier preliminary measurements indicated that the 16-Mev radiation was isotropic with respect to the beam. Since the ground state of  $\text{C}^{12}$  has zero angular momentum, the 16-Mev gamma ray cannot be emitted from a level of  $J = 0$ . Thus the isotropy with the beam would necessitate  $S$ -wave capture. On the other hand, the 12-Mev gamma ray being nonisotropic with the beam requires at least  $P$ -wave capture with  $D$ -wave capture being very improbable.

The answer to the following two questions was therefore sought: (1) Is the 16-Mev angular correlation with the beam not really isotropic but merely small? (2) Do the 16- and 12-Mev radiations actually come from different, but close lying, energy levels? To answer the first question, the yields of the 12- and 16-Mev gamma rays at 180 and 90° with the beam were measured simultaneously by using two spectrometer channels. One channel picked the 12-Mev gamma-ray pulses and the other channel picked the 16-Mev gamma-ray pulses from the same crystal. The result was that the 12-Mev gamma ray showed 16% more anisotropy in the forward direction than the 16-Mev gamma ray. This,

(1) Walker, R. L., "Gamma-Ray Spectra from  $\text{B}^{10}$ ,  $\text{B}^{11}$ , and  $\text{Be}^9$  Under Proton Bombardment," *Phys. Rev.* 79, 172 (1950).

combined with the fact that the anisotropy of the 12-Mev gamma ray is itself about 16% in the forward (and backward) direction, confirms the belief that the anisotropy of the 16-Mev gamma ray is at most a few percent.

To examine the possibility of two different but closely spaced levels giving rise separately to the 12- and 16-Mev radiations, simultaneous yields were taken of the 12- and 16-Mev radiations by again using two spectrometer channels on the same crystal. The results are shown in Fig. 4. It is concluded that if two different levels are involved, they are less than a kilovolt apart.

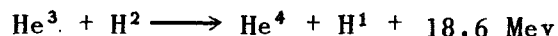
**Scintillation-Counter Gamma-Ray Spectra** (G. Robinson, C. D. Moak, and W. M. Good). A scintillation-counter spectrometer study is being made of the gamma rays from the capture of protons by  $H^2$  and  $H^3$ . These reactions have  $Q$  values of 5.48 and 19.7 Mev, respectively. Since the mass differences of these two reactions are known to small fractions of a milli-mass unit, they should serve as calibration points for the spectrometer.

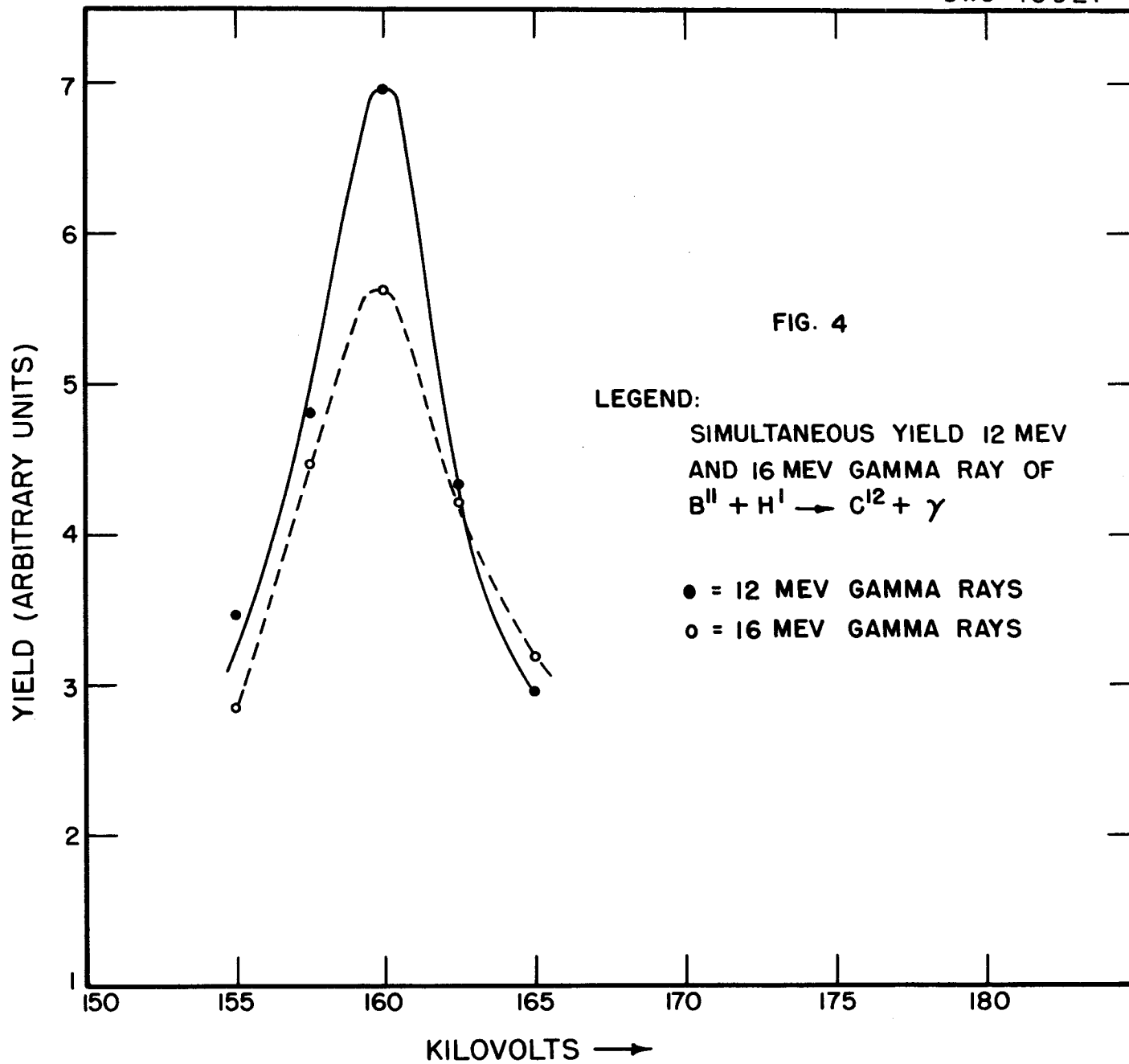
A careful study of the  $B^{11} + H^1$  spectrum is shown in Fig. 5. The 16-Mev gamma ray is not included because the yield is so much lower than that of the 12-Mev gamma ray that its shape is not yet known with comparable accuracy. From the existing values for the precise energies of the two gamma rays, it might appear that the spectrometer falls a few percent short of being linear at the higher energy. Since, however, the zero is not well defined, the question of strict linearity awaits the study of other gamma rays of known energy.

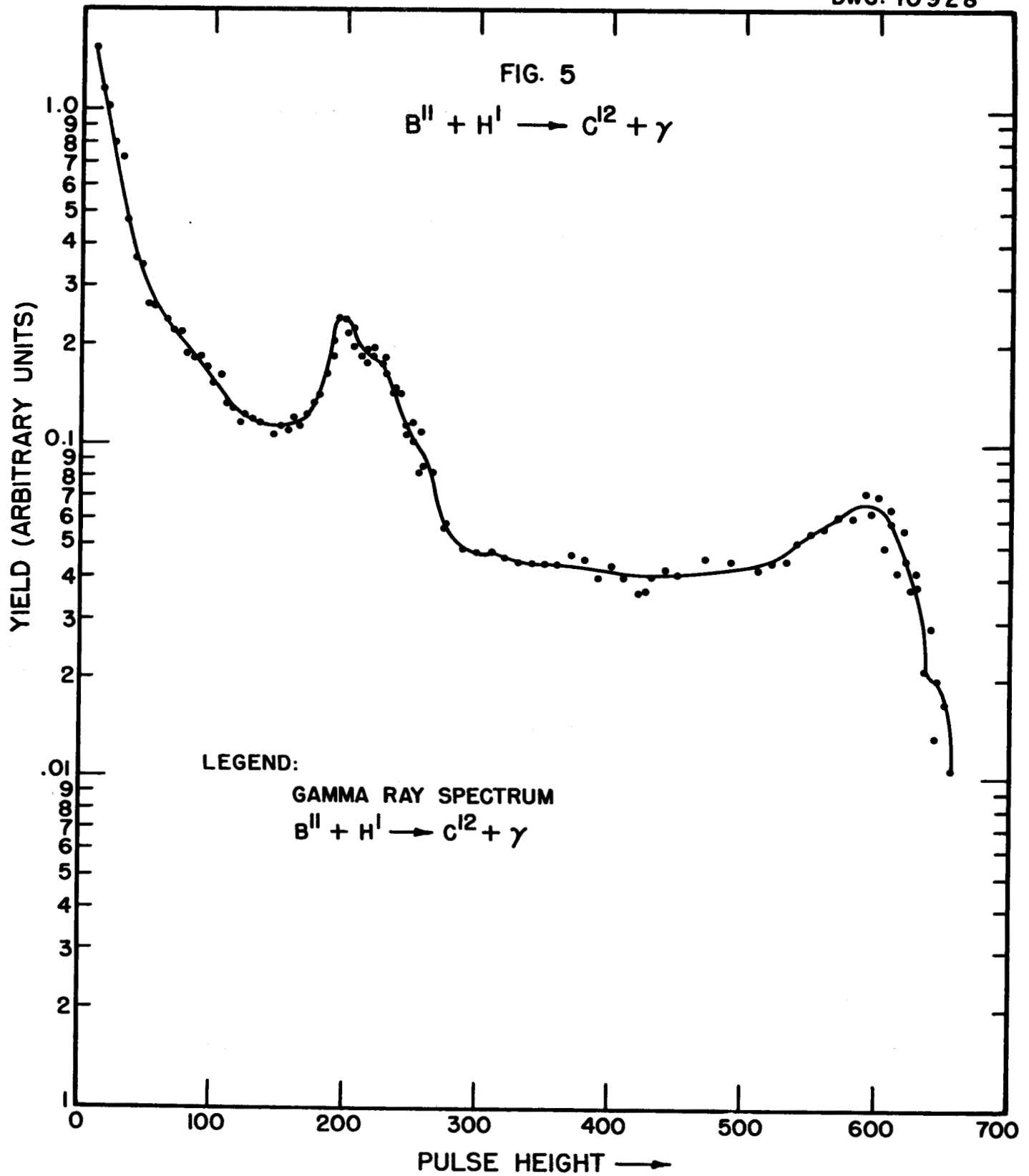
Target difficulties have so far prevented a careful study of the  $H^2 + H^1$  and  $H^3 + H^1$  gamma rays, but Figs. 6 and 7 show the results so far obtained. These data cannot be used to check the linearity of the spectrometer because no attempt was made between these runs to hold the amplifications constant.

**Reactions with  $He^3$**  (W. E. Kunz and W. M. Good). Apparatus has been constructed to make possible the routine acceleration of  $He^3$ . The apparatus consists of special Toepler pumps to back up the oil diffusion pumps for conserving the gas, together with a gas regulator to maintain constant gas pressure in the ion source against a variable supply pressure.

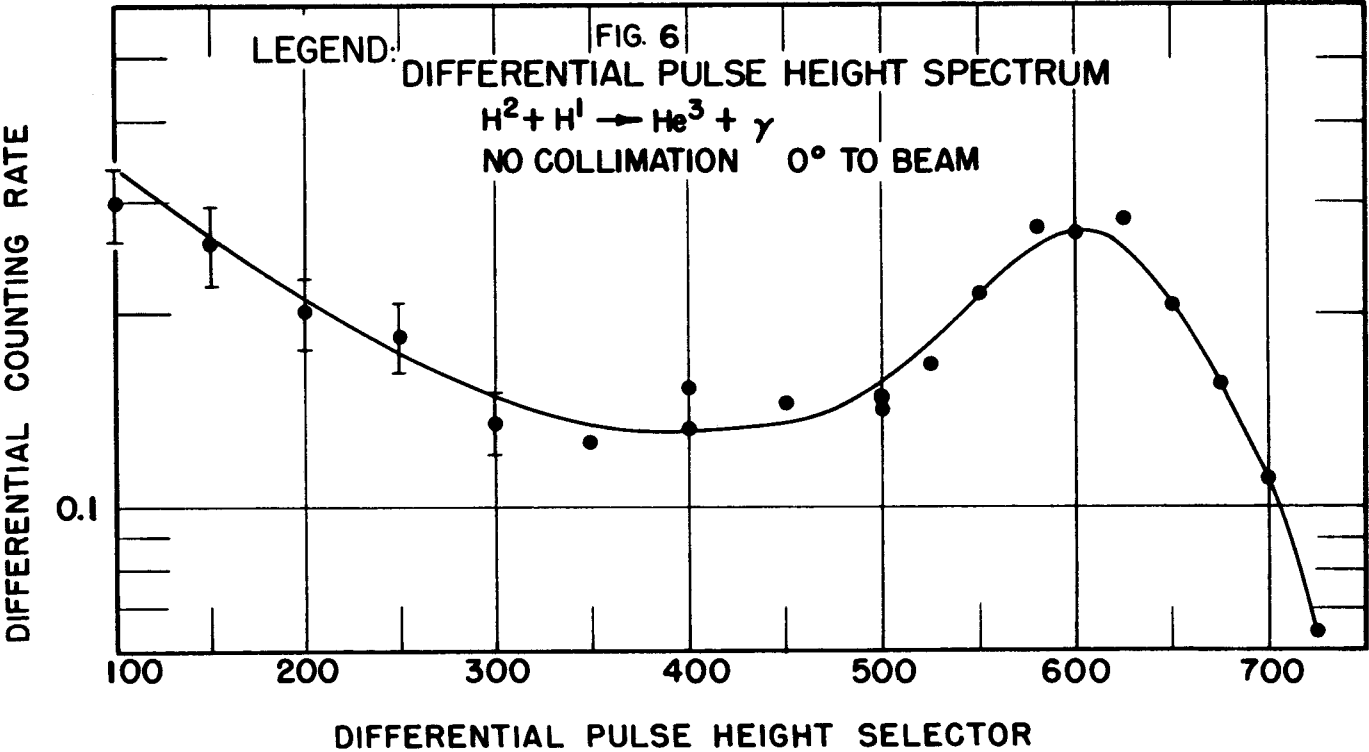
The reaction

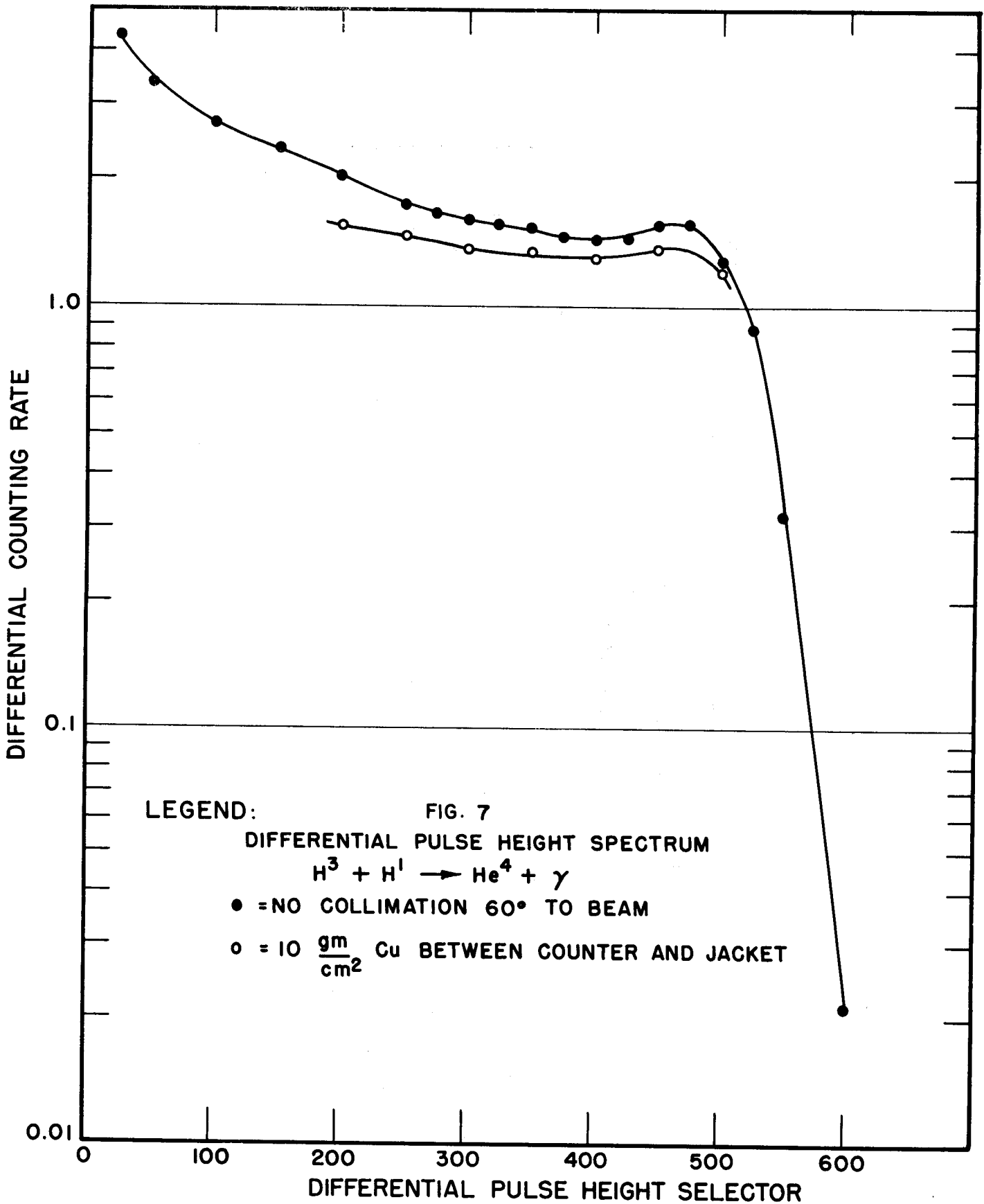






UNCLASSIFIED  
DWG. 10968

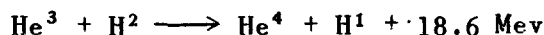




has been studied by other investigators.<sup>(2,3)</sup> The object of this study is to make a careful comparison of this reaction and the reaction

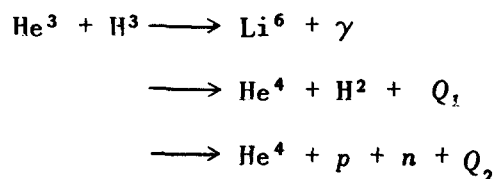


in the range up to a few hundred kilovolts. The reaction



has been identified by its long-range protons. The thick target yield is shown in Fig. 8. Using a "thick" target on a thin backing, a preliminary investigation has been made of the angular distribution of the protons relative to the direction of the beam. The first tentative results are shown in Fig. 9.

Very preliminary indications of the reaction



have been obtained in the form of radiation that produces counts in the scintillation spectrometer and radiation that produces counts in an argon-filled proportional counter. The radiations have not yet been identified.

**Inelastic Scattering of Neutrons** (H. B. Willard and J. Kington). A preliminary experiment investigating the inelastic scattering of fast neutrons has been carried out. Monoenergetic neutrons (14 Mev) were produced by bombarding a thick target of tritium (absorbed in zirconium) with 150-Kev deuterons (100  $\mu\text{a}$ ). The inelastic scattering in lead was studied using the arrangement shown in Fig. 10. The neutrons incident upon the cubes are scattered (elastically and inelastically) into the photographic plate detectors (Ilford C-2 emulsions, 100  $\mu$ ). The shadow cone is used to reduce the directly incident neutron beam. However, since the plates are located at 90°, this attenuation is not entirely necessary and future experiments will determine the relative merits of a shadow cone vs. no cone. Two exposures of the plates were made, with and without the two lead cubes, both of 100  $\mu\text{a}$ -hr duration.

- (2) Wily, L. D., Sailor, V. L., and Ott, D. G., "Protons from the Bombardment of  $\text{He}^3$  by Deuterons," *Phys. Rev.* 76, 1532 (1949).  
 (3) Hatton, J. I. and Preston, G., "Long-Range Protons from the  $\text{He}^3(d,p)\alpha$  Reaction," *Nature* 164, 143 (1949).

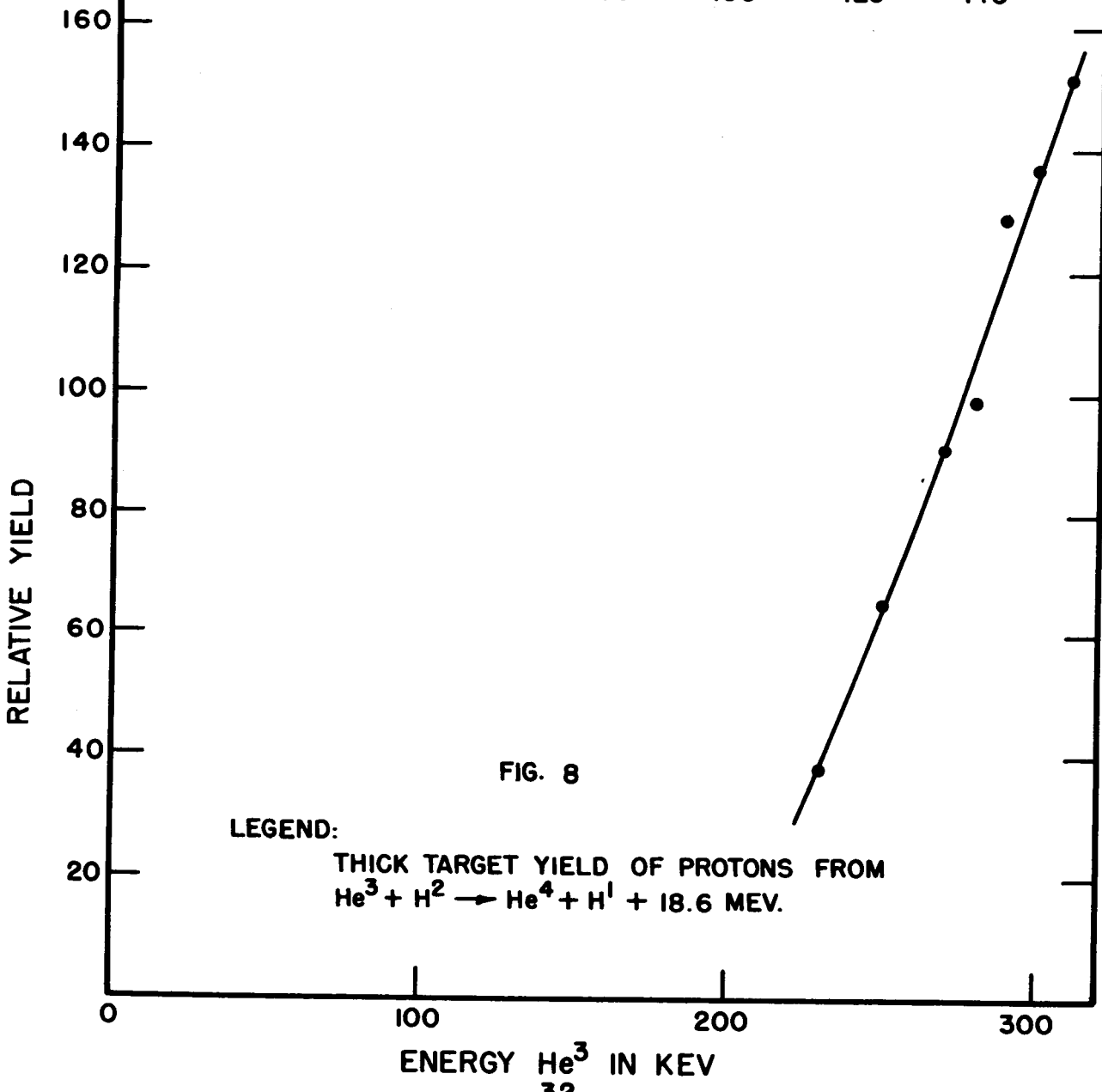
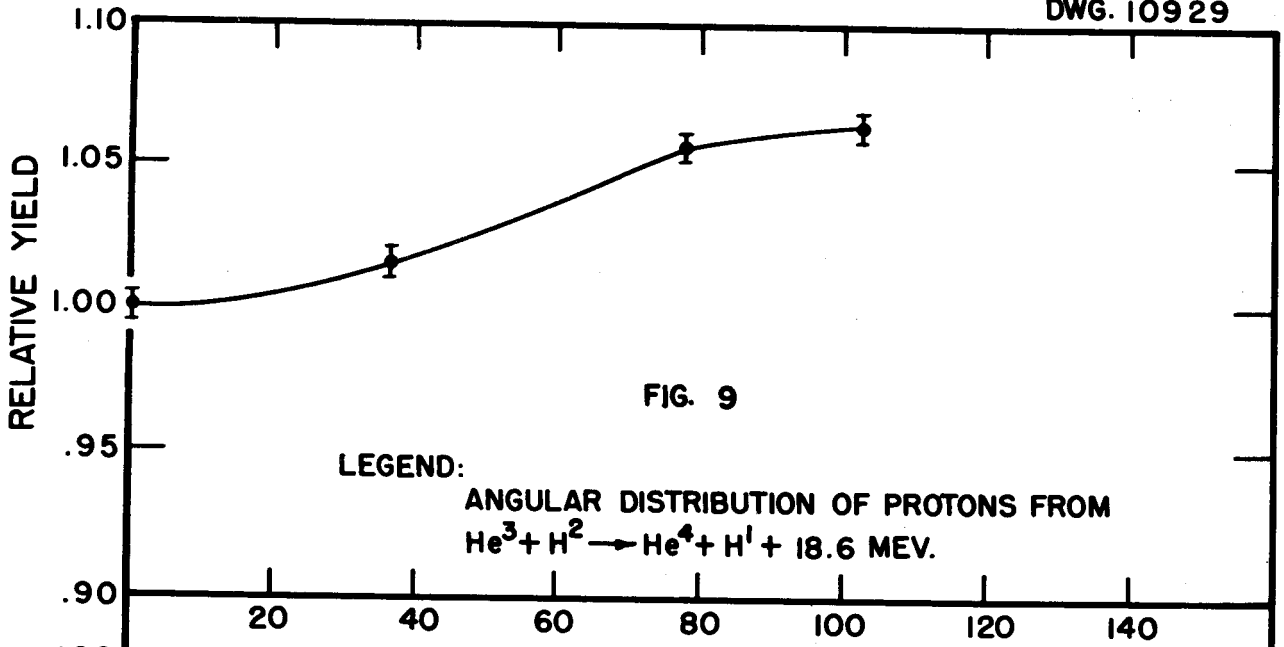
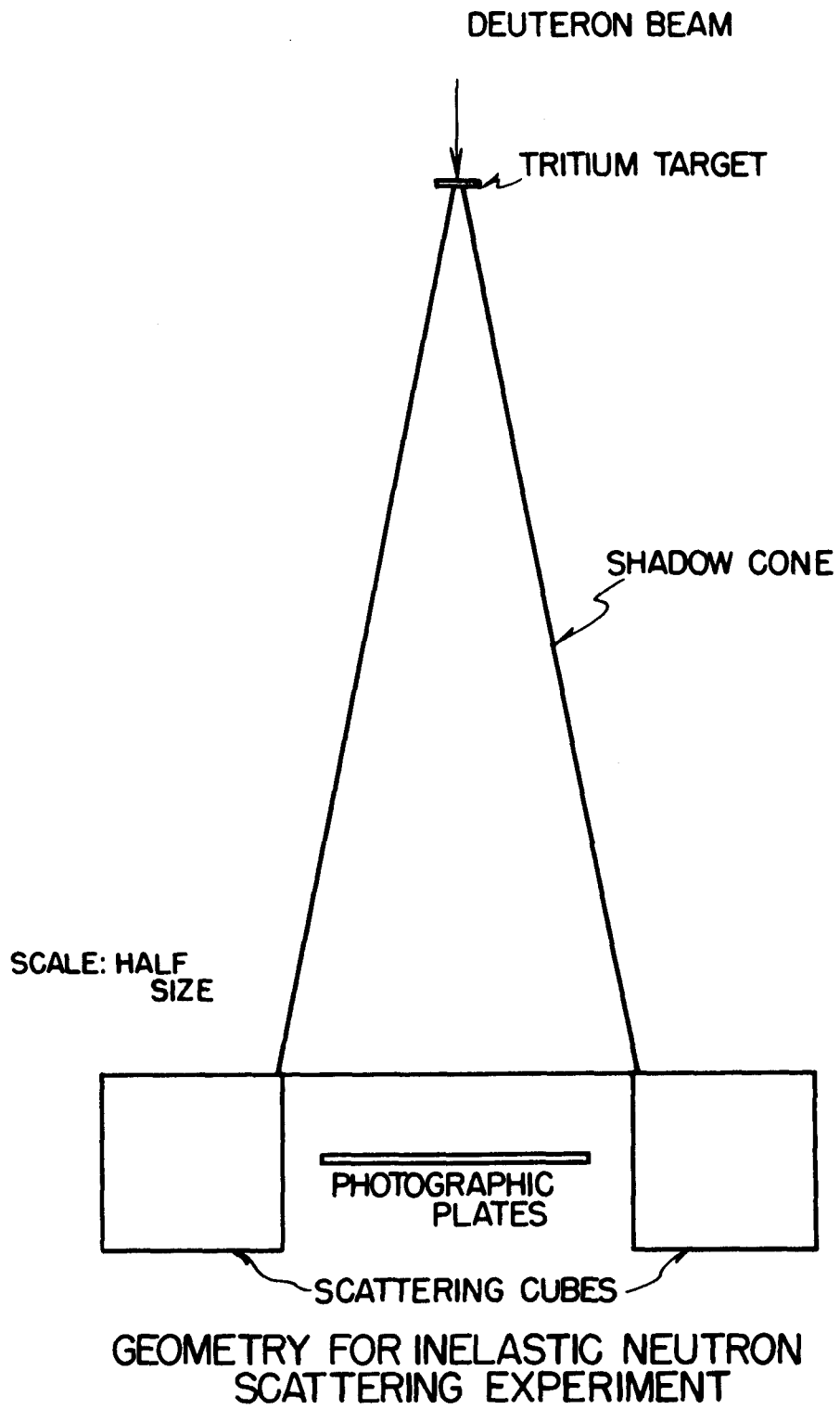


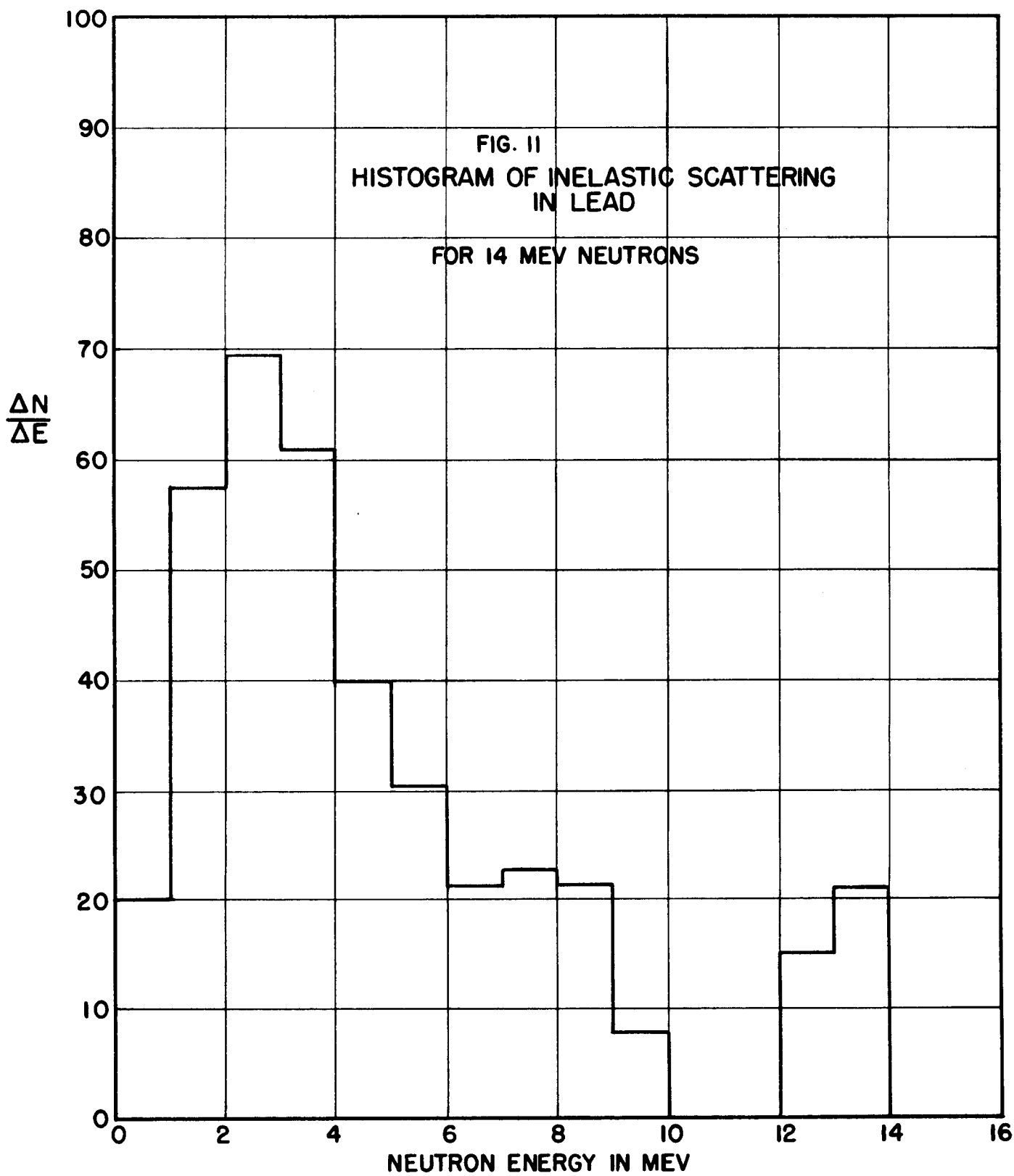
FIG. 10



Thus far 500 tracks from the plates exposed with the cubes present and 100 tracks due to background have been measured. Only those tracks which made an angle of less than  $20^\circ$  with respect to the line joining the centers of the two cubes were accepted. The resultant distribution of neutrons is shown in Fig. 11, where corrections have been made for (a) recoil protons ending in the edge of the photographic emulsion, (b) the  $(n,p)$  scattering cross-section, and (c) the conversion from a range interval  $\Delta r$  to an energy interval  $\Delta E$ .

The curve obtained here is in qualitative agreement with that obtained by Stelson<sup>(4)</sup> in a recent experiment of a similar nature. However, our maximum is shifted to a somewhat higher neutron energy. It is felt that Stelson's geometry is such as to allow the neutrons to undergo multiple collisions with the lead nuclei, thus giving a lower maximum.

(4) P. H. Stelson, Ph.D. Thesis, MIT, September, 1950.



## 6. STANDARD PILE

E. D. Klema

A calibration of the Oak Ridge standard graphite pile using the same indium foils used by Haydn Jones in the calibration reported in CP-2804<sup>(1)</sup> and glass-walled Geiger counters was carried out to find the cause of a discrepancy between Jones' work and that done at Argonne. Both sides of the foils were counted in the present measurements, and a difference in the shape of the experimental curve as a result was observed.

The 1-g Ra-Be neutron source used in the standard pile was sent to the Bureau of Standards for measurement of the number of neutrons per unit time emitted by it. The source was compared with a standard neutron source at the Bureau which has not yet been accurately calibrated. It is hoped that this source will be calibrated to  $\pm 2\%$  with the technique already in use. The present calibration is given to  $\pm 10\%$ .

A gas-flow proportional counter has been set up and used to count indium foils. With this counter the diffusion length of thermal neutrons in the standard pile has been measured with two sources arranged to cancel out the first harmonic of the thermal-neutron flux distribution in the pile. The diffusion length has also been measured with a single source on the axis of the pile and Geiger counters. The experimental results have been given to the Mathematics Panel, and they are calculating the corrections to the observed diffusion lengths due to the harmonic terms and to the nonthermal character of the neutron source. The neutron spectrum of the source is being represented by three groups of range 28, 40, and 60 cm, respectively. The fraction of the neutrons in each group has been determined from the present calibration of the standard pile.

A NaI scintillation counter has been set up to count the gamma rays from indium foils in a set of experiments on the perturbation of the thermal-neutron flux due to the presence of indium foils of various thicknesses. It is hoped to use this counter to make an absolute measurement of the gamma rays from a gold foil and to obtain in this way a calibration of the standard pile which is independent of the calibration of the source used in the pile.

(1) Arnette, T., and Jones, H., CP-G-2804 (Apr. 30, 1945).

## 7. HEAVY-ION RESEARCH

G. E. Evans            C. F. Barnett  
P. M. Stier            V. L. DiRito

Work on the behavior of thin evaporated films upon bombardment with 200-Kev protons has been initiated. Thin films of gold have been evaporated on the surfaces of 2S aluminum targets and then bombarded with 200-Kev protons for periods of 3 to 4 hr at about  $20 \mu\text{a}$ . Prior to bombardment, the gold foils were activated by exposure in the X-10 reactor so that the location and number of atoms sputtered from the surface could be determined. Even for the best gold targets, smooth and apparently well bonded to the aluminum before and after bombardment, some spalling of microscopic flakes of gold occurred. In one case a large percentage of the activity of the sputtered material was found to be in particles large enough to be removed by simple filtration. New targets have been prepared, using improved annealing techniques, to see if the stability of the evaporated surface to proton bombardment can be improved.

An electron multiplier for heavy-ion detection has been built and is ready for use. An electrometer tube detector, together with associated electronic equipment, has been built and will be used for the detection of small positive ion currents. Ion-source studies are being continued; three different sources are being tested for output and stability.

## 8. NEUTRON-SENSITIVE PHOSPHORS

J. Schenck

A number of neutron-sensitive phosphors have been prepared in microcrystalline form and their luminescent properties have been observed (Table 1). All the phosphors contained a large amount of lithium to bring about luminescence emission from excitation by the products of the  $\text{Li}^6(n,\alpha)\text{H}^3$  reaction. The luminescent compounds prepared were limited to those containing oxygen. They were prepared by reaction at an elevated temperature of the component dry oxides, acids, or carbonates.

In the cases of lithium and calcium tungstate it was found necessary to add a slight excess (0.5%) of lithium or calcium carbonate to ensure a complete reaction of the tungstic acid. It was found that crystals of unactivated lithium tungstate were not luminescent until they had been crushed in a mortar.

Lithium and calcium carbonates were prepared by precipitation from purified lithium or calcium chloride with distilled ammonium carbonate. Tungstic acid was precipitated by nitric acid from purified sodium tungstate. The silica, titania, and zirconia were found to be sufficiently pure to start with.

All the tests for alpha excitation were made at room temperature with an RCA ultraviolet-sensitive No. C7140 photomultiplier. A thin layer of the phosphor powder on a micro cover glass was supported between the photocathode and alpha source. No tabulation is given for excitation by neutrons since the energy of the polonium alpha particles is near enough to that expected from the absorption of neutrons by  $\text{Li}^6$ . This was confirmed at times during the tests using a moderated Po-Be neutron source. A special test with neutrons was made with  $\text{Li}_2\text{Si}_2\text{O}_5:\text{Ti}$ , a quarter-inch translucent slab of which was obtained by slowly cooling the melt. The slab gave a neutron counting efficiency of 40% relative to an assumed 100% efficiency of a calibrating enriched- $\text{BF}_3$  proportional counter.

Although  $\text{Li}_2\text{Si}_2\text{O}_5:\text{Ti}$  is an efficient phosphor, its relatively long decay time is a disadvantage. Consequently an effort has been made to find phosphors of shorter decay time. Cerium-activated  $\text{Li}_2\text{CaSiO}_4$  has the shortest decay of those found (less than  $0.2 \mu\text{sec}$ ). It responds very strongly to ultraviolet

TABLE 1

Response of Some Lithium- and Oxygen-Containing Phosphors  
to Ultraviolet and Alpha Particles

PHOSPHOR			RESPONSE					
COMPOUND	IMPURITY		ULTRAVIOLET EXCITATION				POLONIUM ALPHA EXCITATION	
	(mole %)	SUBSTANCE	3650 A		2537 A		INTENSITY	DECAY TIME CONSTANT ( $\mu$ sec)
			INTENSITY*	COLOR**	INTENSITY*	COLOR**		
Li <sub>2</sub> SiO <sub>3</sub>	10	Ti			M	R-W	M	200
Li <sub>2</sub> SiO <sub>3</sub>	3	Ta			M	W	M	200
Li <sub>2</sub> SiO <sub>3</sub>	4	Sn			S	B	M	200
Li <sub>2</sub> SiO <sub>3</sub>	1	Sb			M	B	S	200
Li <sub>2</sub> Si <sub>2</sub> O <sub>5</sub>	5	Ti			S	Y-W	S	200
Li <sub>2</sub> Si <sub>2</sub> O <sub>5</sub>	3	Ta			S	W	VW	100
Li <sub>2</sub> Si <sub>2</sub> O <sub>5</sub>	4	Sn			W	V		
Li <sub>2</sub> Si <sub>2</sub> O <sub>5</sub>	1	Sb			W	V	M	200
Li <sub>2</sub> CaSiO <sub>4</sub>	1	Sb			W	V	W	50
Li <sub>2</sub> CaSiO <sub>4</sub>	5	Ce	S	B	VS	B	M	<0.2
Li <sub>2</sub> TiO <sub>3</sub>	1	Mn	M	R	W	R		
Li <sub>2</sub> Ti <sub>2</sub> O <sub>5</sub>	1	Mn	M	R	W	R		
Li <sub>2</sub> TiSiO <sub>5</sub>					M	W		
Li <sub>4</sub> ZrO <sub>4</sub>			W	V	M	B-W	S	2
Li <sub>2</sub> ZrO <sub>3</sub>			W	V	M	B-W	S	2
Li <sub>2</sub> Zr <sub>2</sub> O <sub>5</sub>			W	V	M	B-W	S	2
Li <sub>2</sub> ZrSiO <sub>5</sub>			VW	W	S	W	M	100
Li <sub>2</sub> ZrTiO <sub>5</sub>			M	W	S	W	S	4
Li <sub>2</sub> CaZrO <sub>4</sub>					M	V		
Li <sub>2</sub> CaZrO <sub>4</sub>	1	Pb			M	R-V		
ZrO <sub>2</sub>			W	V	S	W	M	2
CaWO <sub>4</sub>					VS	B	S	10
Li <sub>2</sub> WO <sub>4</sub>					M	W		
Li <sub>2</sub> WO <sub>4</sub>		Pb			W	W		

\*VS, very strong; S, strong; M, medium; W, weak; VW, very weak.

\*\*R, red; Y, yellow; B, blue; V, violet; W, white.

excitation and has a moderately strong, and probably improvable, response to alpha particles. The decay of luminescence is characterized by the superposition of a much weaker decay of about 50  $\mu$ sec. The cerium activator must be incorporated in the lower valence state (III), and for this reason the phosphor must be prepared in either a neutral or reducing atmosphere. It is possible that the long-decay component was caused by some cerium that has been oxidized to the IV state.

The zirconium compounds, including zirconia, generally exhibit a strong emission under ultraviolet or alpha-particle excitation and do not require the incorporation of an activator impurity. Except for  $\text{Li}_2\text{ZrSiO}_5$ , the decay times are short enough for most applications involving neutron excitation. It has been found, however, that the melting point of these zirconates is too high for the growing of large crystals from the melt with a conventional furnace. It is possible that crystals of the zirconates of sufficiently large size could be made by the Verneuil method.

The data reported here are in connection with the problem of neutron detection and also of neutron-energy-spectrum measurements by means of scintillation techniques. The requirements of the latter application are met by a sufficiently large transparent crystal of a suitable phosphor. For the purpose of growing large crystals, apparatus has been constructed to determine the crystal-growth properties of phosphors and to grow large crystals from the melt. The crystal-growing furnace provides a cylindrical hot zone 2 in. in diameter and 8 in. long. Heat is supplied to the top and bottom halves of the cylinder by two separately controlled, internally wound, Pt-10% Rh resistance-heater coils. The melt is contained in the 0.001-in.-thick platinum liner of a ceramic crucible, 1½ in. in diameter and 3 in. long, with a conical bottom of 60° apex. The crucible is supported by a ceramic rod which is joined to a metal rod and connected through a gear drive and speed control to a synchronous motor. The crucible may be lowered out of the hot zone at any desired speed. By means of automatic temperature control the lower half of the resistance heater maintains the temperature within 0.5°C in the neighborhood of the surface where crystal growth occurs.

The furnace has been tested by lowering a melt of  $\text{Li}_2\text{SiO}_3$  (m.p. 1201°C) out of the hot zone over a 24-hr period. The results proved that the furnace construction was satisfactory but that a much lower rate of lowering was necessary for this compound.

The temperature-control circuit can be connected to a smaller oven where the crystallization characteristics of different phosphor compositions can be more completely determined. In this arrangement the melt is cooled automatically at a constant rate in a small platinum cone, at the tip of which is welded a Pt, Pt-10% Rh thermocouple. As the oven cools, chart records are obtained of the temperature of the cone and also of the temperature difference between the cone and the oven.

It is planned to install a combustion tube in the crystal-growing furnace in order to grow crystals in a controlled atmosphere. This alteration is necessary for an attempt to grow LiI:Tl. A special atmosphere is also required for cerium-activated phosphors.

## 9. SHORT-PERIOD ACTIVITIES

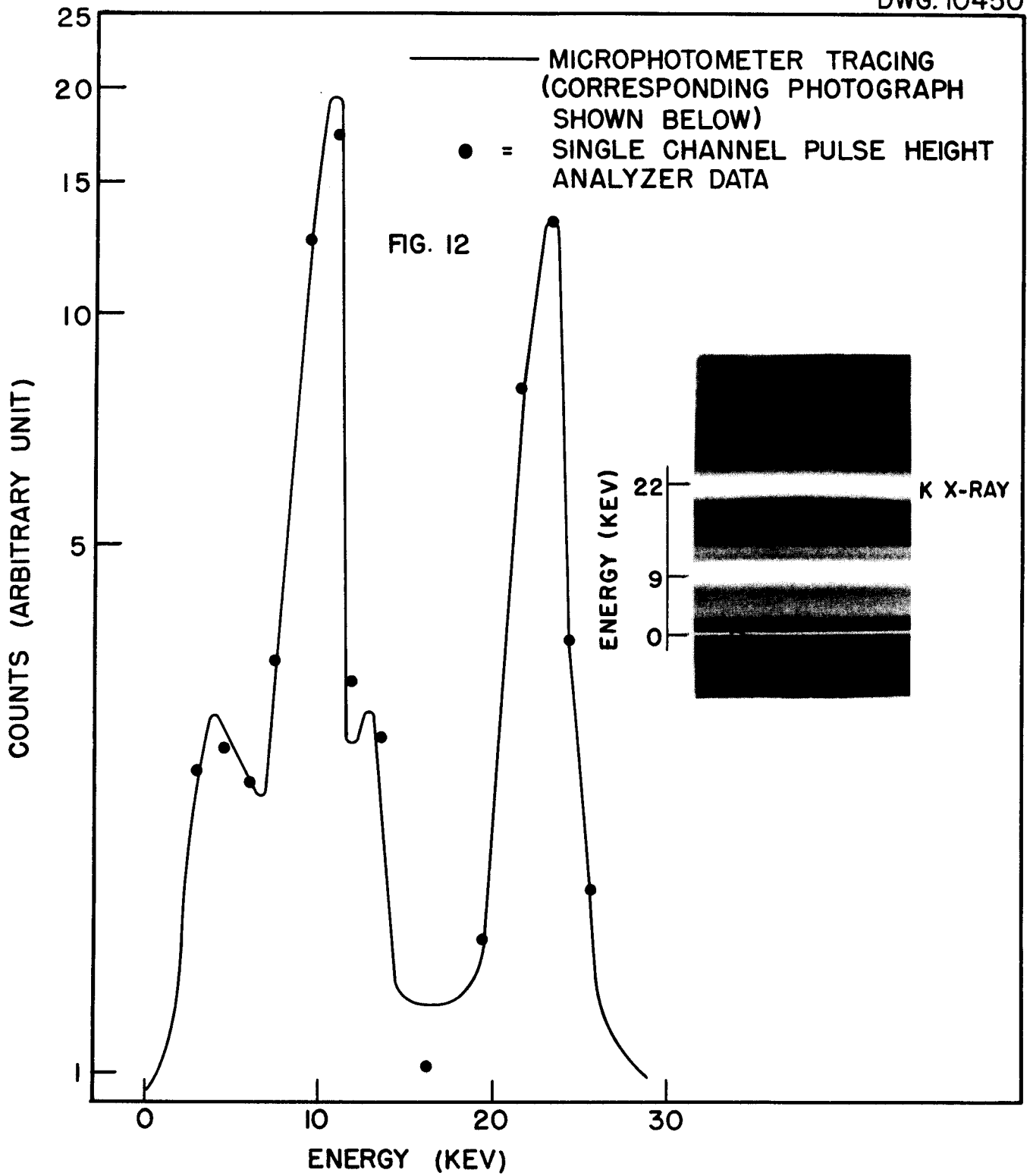
### Pulse Analyses by Photographic Densities (E. C. Campbell and J. H. Kahn).

The pulse analysis obtained using a photographic-density technique<sup>(1)</sup> has been compared with that obtained using the Fairstein pulse-height analyzer.<sup>(2)</sup> The X rays from Cd<sup>109</sup> (330-day) as detected by a krypton-methane filled proportional counter are shown in Fig. 12. According to Bradt *et al.*<sup>(3)</sup> Cd<sup>109</sup> decays by K capture to an isomeric state of Ag<sup>109</sup> (39.2-sec) with the subsequent emission of an 89-Kev gamma ray that is highly converted. Ag K X-rays will be produced by the capture of the K electrons in Cd<sup>109</sup> and by the emission of K conversion electrons from Ag<sup>109</sup>. The conversion electrons are stopped by the counter walls, and the counter efficiency is too low to detect any unconverted gamma rays. The L X-rays are too soft (approximately 3 Kev) to be observed above background noise.

Whenever an Ag K X-ray produces a photoelectron from the K shell of the krypton, either of two processes may occur; the ionized krypton atom will either emit (1) one or more Auger electrons or (2) its characteristic K X-ray. If the Auger process occurs, the entire energy of the incident X ray is spent in the counter, and this produces the high-energy peak shown in Fig. 12. If a K X-ray is emitted by the krypton, it has a good probability of escaping from the counter and thus part of the energy of the incident X ray is lost, which accounts for the lower peak shown in Fig. 12. Its energy is less than that of the incident X ray by an amount equal to the krypton K X-ray energy (13 Kev). It should be pointed out that following the emission of a K X-ray in the krypton there may be L, M, etc. X rays emitted as well as Auger electrons from these levels, but these are readily absorbed within the counter. Likewise, in the event that the initial photoelectron comes from outside the krypton K shell, any subsequent radiation will be absorbed in the counter and produce a pulse equivalent in energy to the incident radiation.

The resolution of this instrument as measured by the ratio of peak width at one-half maximum intensity to peak energy is from 14 to 18%. This is not sufficient to differentiate between the Ag K $\alpha$  and K $\beta$  peaks in Fig. 12. When a

- (1) Campbell, E. C., and Kahn, J. H., in *Physics Division Quarterly Progress Report for Period Ending September 20, 1950*, ORNL-865, p. 16 (Jan. 8, 1951).
- (2) Fairstein, E., *A Sweep Type Differential and Integral Discriminator*, ORNL-893 (Feb. 12, 1951).
- (3) Bradt, H., Gugelot, P. C., Huber, O., Medicus, H., Preiswerk, P., Scherrer, P., and Steffen, R., "Die metastabilen Zustände der Silberkerne Ag<sup>107</sup> und Ag<sup>109</sup>," *Helv. Phys. Acta.* 20, 153 (1947).



X-RAYS FROM Cd<sup>109</sup> (330 d) AS DETECTED BY KRYPTON  
METHANE FILLED PROPORTIONAL COUNTER

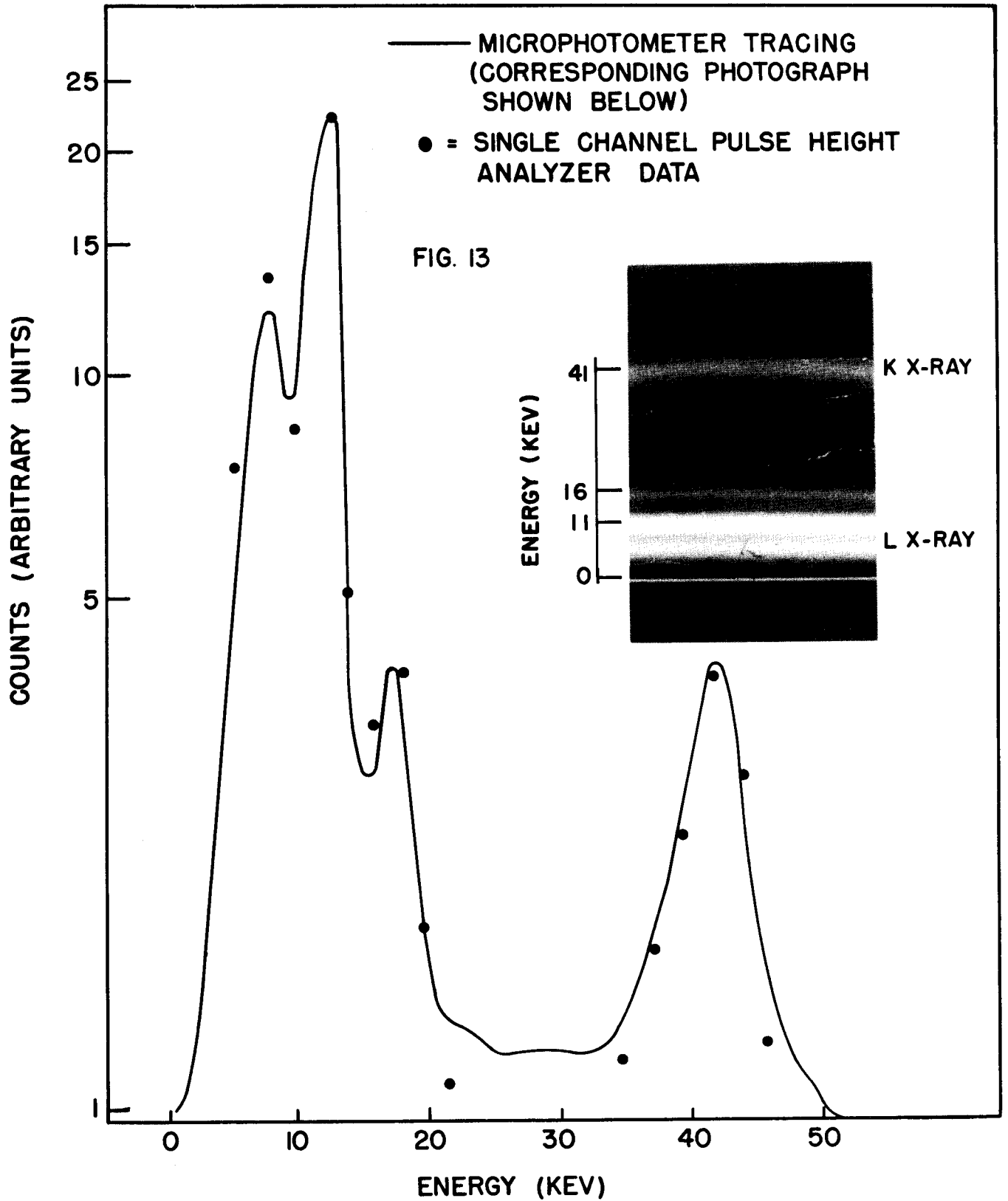
constant energy is subtracted from the incident  $K\alpha$  and  $K\beta$  radiation (owing to the escape of a Kr K X-ray) the percent difference between the  $K\alpha$  and  $K\beta$  lines is increased and these two lines can be resolved. The satellite just above the peak at 10 Kev is caused by the absorption of an Ag  $K\beta$  X-ray and the subsequent escape from the counter of a Kr K X-ray.

The total number of counts registered in making the photograph shown in Fig. 12 is over  $10^5$ . The maximum number of counts per channel per minute, using the pulse-height analyzer, was about  $1.7 \times 10^4$ . The pulse-height analyzer data were superposed on the microphotometer tracing by normalizing the data so that the more energetic peak heights coincided.

In Fig. 13 are shown the X rays from  $\text{Eu}^{152}$  (9.2-hr) as detected by a xenon-methane filled proportional counter. According to Muehlhause<sup>(4)</sup>  $\text{Eu}^{152}$  decays by K capture as well as through beta and gamma emission. Sm K X-rays will be produced by the capture of K electrons in  $\text{Eu}^{152}$ , and there will probably be other X rays produced by the internal conversion of some of the gamma rays. A 1-cm thickness of beryllium was placed between the source and the counter in order to absorb all the beta radiation which would otherwise obliterate the X-ray spectra. The peak at 41 Kev is due to the absorption of the total energy from the incident K X-rays. As stated before, the resolution of the spectrometer is not sufficient to resolve the  $K\alpha$  and  $K\beta$  X-rays directly. The peak at 11 Kev is caused by the detection of the incident  $K\alpha$  radiation and the subsequent escape of Xe K X-rays. The less intense peak at 16 Kev results from the detection of the  $K\beta$  radiation followed by the escape of the Xe K X-ray. The 6.5-Kev peak is caused by the incident L X-rays as the relative height of this peak is decreased by interposing thicker absorbers between the sample and the counter. Over  $2 \times 10^5$  counts were registered while exposing the photograph shown in Fig. 13, and the maximum number of counts per channel per minute registered with the pulse-height analyzer was about  $1.5 \times 10^4$ .

Figures 12 and 13 indicate that the pulse analyses obtained from photographic densities are comparable to those obtained from single-channel pulse-height analyzer data. The density method has the advantage of being less

(4) Muehlhause, C. O., in *Report for October, November, and December, 1946*, Argonne Report CP-3750, p. 46 (Jan. 17, 1947).



X-RAYS FROM  $\text{Eu}^{152}$  (9.2 hr.) AS DETECTED BY  
XENON-METHANE FILLED PROPORTIONAL COUNTER

laborious and better adapted for studying short-period activity, but for accurate results densities must be limited to the linear portion of the characteristic (density vs. log exposure) curve of the film.

**Fermi Plots of  $\text{Ag}^{110}$  (24-sec) and  $\text{Ag}^{108}$  (2.4-min) Beta Spectra** (Max Goodrich\*). In the last quarterly report (ORNL-940) a Fermi plot of the beta spectrum of  $\text{Ag}^{108}$  was given with an approximate analysis into two groups with end points at 0.83 and 1.48 Mev. In Fig. 14 is shown the more exact analysis of the same data. A similar curve, Fig. 15, is given of the beta spectrum of 24-sec  $\text{Ag}^{110}$ . The best values of the maximum energies are:

$\text{Ag}^{110}$	2.24 Mev and 2.82 Mev
$\text{Ag}^{108}$	1.48 Mev and 1.05 Mev

\*Research Participant, Oak Ridge Institute of Nuclear Studies; on leave from Department of Physics, Louisiana State University.

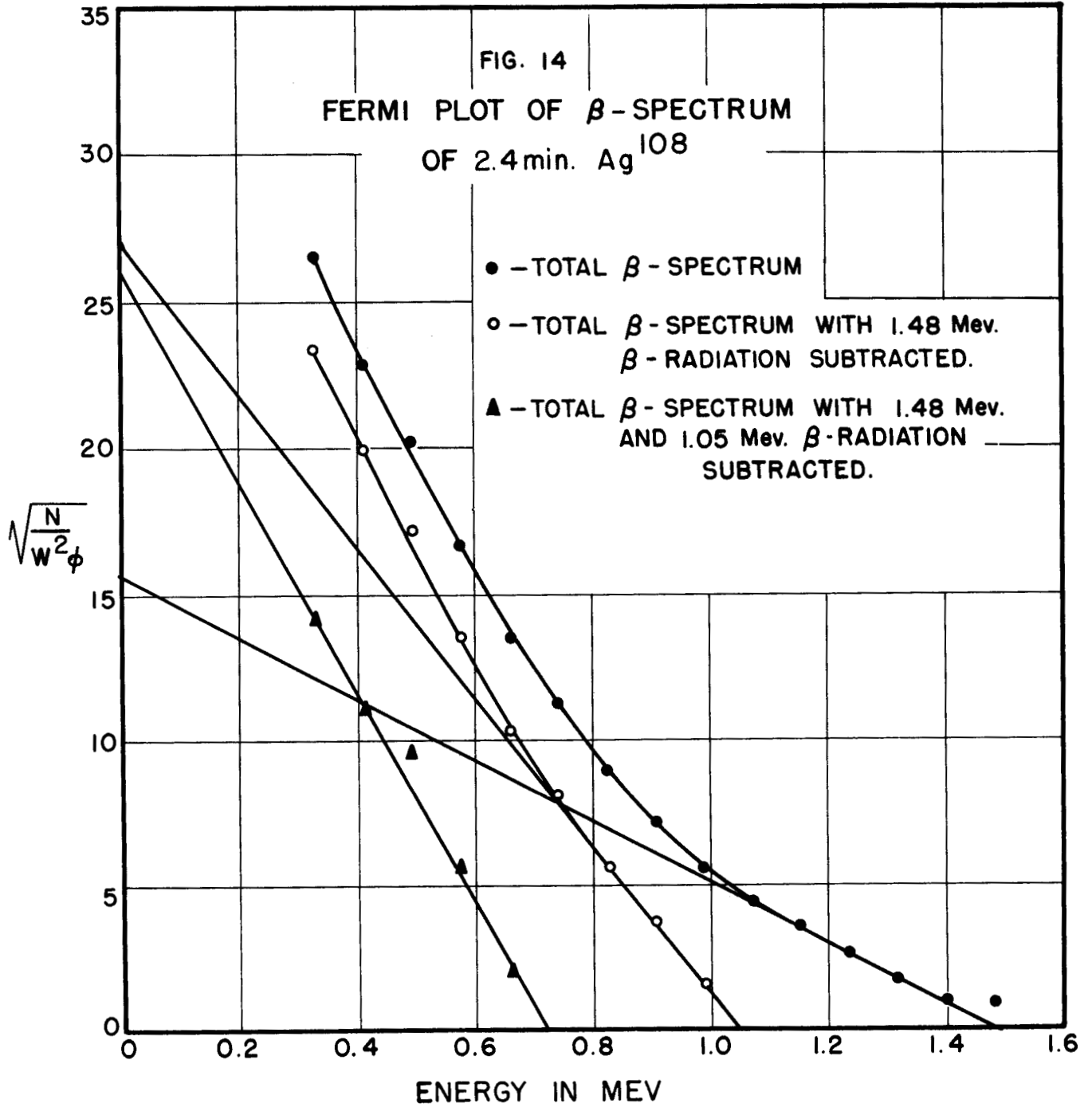
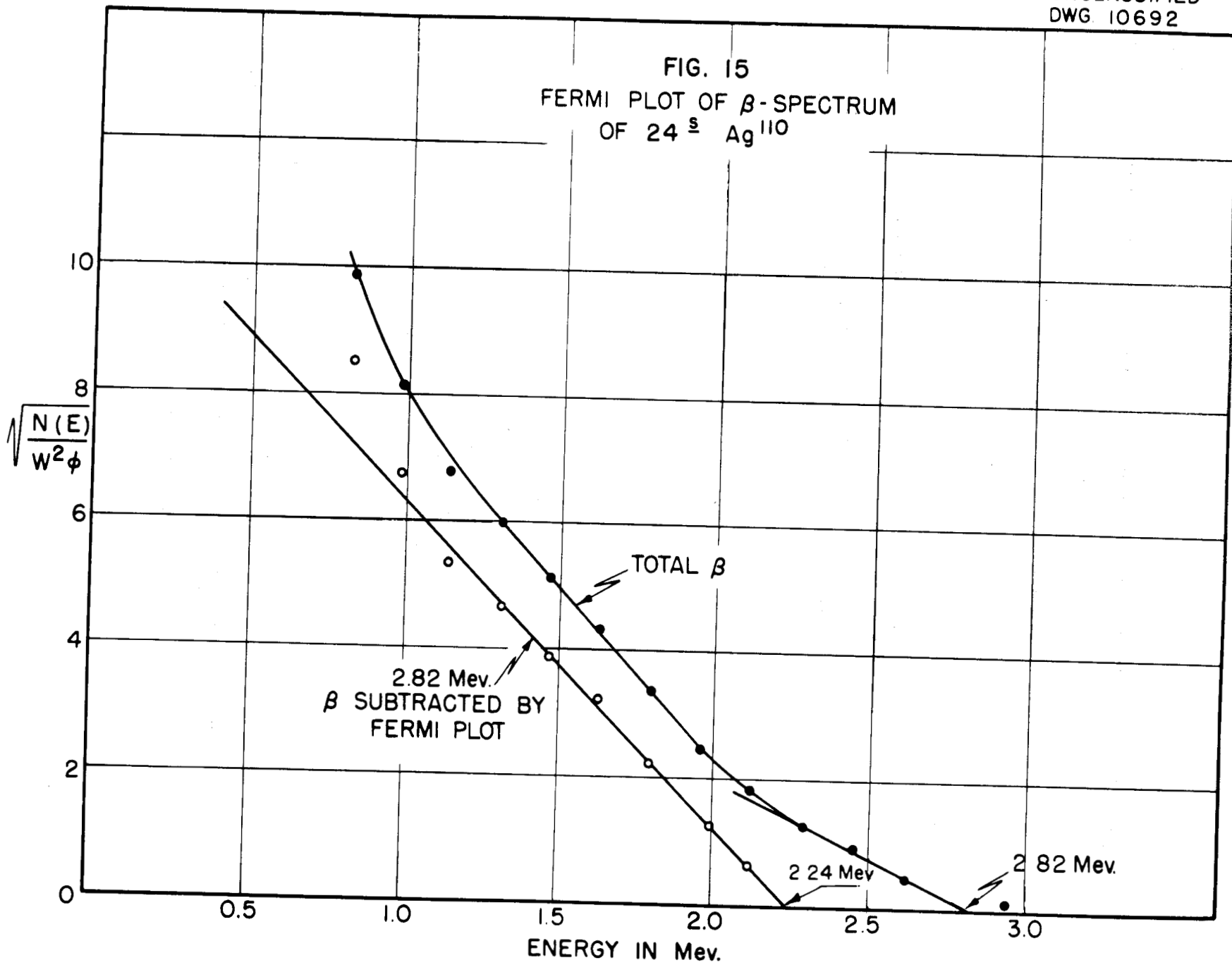


FIG. 15  
FERMI PLOT OF  $\beta$ -SPECTRUM  
OF  $^{24}_{\text{Ag}}^{110}$

-48-



## 10. LONG-WAVELENGTH NEUTRONS

R. G. Allen

During the past quarter preliminary experimental work was done using a plane pyrex mirror to reflect neutrons with the view of establishing the feasibility of using the critical-angle properties of such mirrors to eliminate higher order Bragg reflections from a single crystal while maintaining a usable intensity.

A partial survey of the intensity of Bragg reflections at 2.3 and 2.8 Å for various crystals was carried out in order to discover a crystal giving a maximum intensity in the diffracted beam and still possessing a reasonable resolution, i.e., of the order of 10' to 20' of arc.

From the results of this work it was decided that the use of mirrors in this way in conjunction with a quartz crystal was practical, and apparatus for this purpose was designed and its construction started.

This neutron source can be used for accurate determinations of total cross-sections at these low energies. Coherent scattering cross-sections can also be determined from the heights of the discontinuities in the total cross-section vs. energy curve. We are especially interested, if available intensities permit, in studying the polarization of these low-energy neutrons on passage through magnetized iron. Such data may give a much more accurate value for the form factor of the 3d shell in iron than is now available.

## 11. THEORETICAL PHYSICS

M. E. Rose            L. C. Biedenharn  
T. A. Welton        A. Simon  
G. B. Arfken        S. Tamor  
                      F. G. Prohammer

As the scope and effort of the theoretical group expands it seems worthwhile to summarize the various unclassified projects currently engaging the interest of the members of the group. These are listed below with an indication of their status. Those items marked by an asterisk involve fairly large-scale computational work which, with one exception (L-shell internal conversion), is being carried out by the Mathematics Panel.

- \*1. L-shell internal conversion (M. E. Rose). This work is being carried out on the SEAC at the Bureau of Standards in Washington.
- \*2. K-shell internal-conversion interpolation (M. E. Rose). This work is nearing its final stages on the IBM machines. A paper containing the machine (Mark I) results has been submitted to *Physical Review*.
- \*3. Fermi functions for forbidden beta decay (M. E. Rose and P. R. Bell). This work is in progress on the IBM machines.
- \*4. RaE spectrum and finite size of nucleus (M. E. Rose and D. K. Holmes). This work is in progress on the IBM machines.
- \*5. Angular correlation of internal-conversion electrons and gammas (M. E. Rose and G. B. Arfken). This problem has been set up for computation which has not yet been initiated (see below).
6. Angular correlation of three successive radiations (L. C. Biedenharn, G. B. Arfken, and M. E. Rose). This work is essentially complete (see below).
7. Polarization effects in neutron capture (L. C. Biedenharn, G. B. Arfken, and M. E. Rose). This work is complete (see below).
8. Hyperfine structure in manganese ammonium sulfate (A. Simon). This work is in progress (see below).
- \*9. Mechanism of energy loss of slow ions (S. Tamor). This work is in progress (see below).
10. Neutron-deuteron scattering (T. A. Welton and F. Prohammer). This work is in progress (see below).
11. Theory of neutron scattering (T. A. Welton). This work is in progress (see below).

12. Isotropy of nuclear gamma radiation (G. B. Arfken, L. C. Biedenharn, and M. E. Rose). This work is complete (see below).
13. Symmetry in beta decay (L. C. Biedenharn and M. E. Rose). This work is complete (see below).

**Angular Correlation of Internal-Conversion Electrons and Gammas** (M. E. Rose and G. B. Arfken). In a cascade transition in which either of the two transitions corresponds to a large internal conversion, the most important correlation is the one cited above. The theory was developed by Ling<sup>(1)</sup> but no numerical results could be given at the time. What is needed to get such results has been supplied by the K-shell internal-conversion calculation. The computational problem has been set up for calculation of the correlation for dipole-dipole, dipole-quadrupole and vice versa, and quadrupole-quadrupole cascades where for the transition giving a conversion electron both electric and magnetic transitions will be computed. The energy and  $Z$  values are as for the K-shell conversion calculation.

**Angular Correlation of Three Successive Radiations** (G. B. Arfken, L. C. Biedenharn, and M. E. Rose). We have solved the general problem of determining the coincidence counting rate in a nuclear cascade process for three particles emitted (or absorbed) at arbitrary angles. In particular, the solution applies to the cascade gamma rays that follow the capture of a  $p$  proton by  $B^{11}$ . It has been shown that there are no cross terms from the two channel spins. In general, all cross terms vanish if any two of the radiations are restricted to the same direction of propagation. This gives six special cases, of which the two where one gamma is parallel to the proton beam are of particular interest. The correlation function in general depends upon which gamma is emitted first and so provides a means of determining the order of emission of the gammas. Limits on the possible powers of  $\cos^2 \theta$  have been determined for the general case and for special cases of interest. The formalism covers all cases of polarizations and arbitrary mixtures of multipoles. A detailed report giving proofs and applications to  $B^{11}(p, \gamma\gamma)C^{12}$  is being prepared.

**Polarization Effects in Neutron Capture** (L. C. Biedenharn, G. B. Arfken, and M. E. Rose). When polarized neutrons are captured by a nucleus which subsequently emits gamma radiation, the intensity of the gammas is isotropic

(1) Ling, D. S., dissertation, University of Michigan, 1948.

as long as the neutrons are slow. The question is now: If the radiation is observed with polarization-sensitive detectors, what will be the angular distribution of the radiation? The motivation here is the possibility of obtaining angular momentum and/or parity information with regard to the compound-nucleus energy states. Since the known detectors can be used for the observation of linear polarization only, it turns out that for both pure and mixed multipoles the radiation is isotropic and independent of the neutron polarization. Therefore, using slow neutrons in an experiment of the type envisaged will yield no results of interest beyond what could be obtained with an unpolarized beam. A different conclusion would apply if it were possible to devise a "nuclear quarter-wave plate." A report describing the problem and its solution in detail has been prepared.

**Hyperfine Structure in  $Mn^{++}$**  (Albert Simon). The existence of a hyperfine structure (hfs) in the solid state has been demonstrated by microwave resonance methods.<sup>(2)</sup> The possibility of using this interaction to produce nuclear alignment was first pointed out by Rose<sup>(3)</sup> and by Gorter,<sup>(4)</sup> and an experimental effort is now underway at this Laboratory in an effort to obtain nuclear alignment in manganese ammonium sulfate. Bleaney<sup>(5)</sup> has measured the hfs coupling in  $Mn(NH_4)_2(SO_4)_2 \cdot 6H_2O$  and found that it is given by

$$\Delta W_{hfs} = A I \cdot S$$

where  $I$  is the nuclear spin (5/2) and  $S$  the electronic spin (5/2) in manganese. The magnitude of  $A$  was determined to be  $0.009 \text{ cm}^{-1}$  but no determination of the sign of  $A$  has been published as yet.

A knowledge of the form of the hfs is essential in order to compute the optimum magnetic field for nuclear alignment in adiabatic demagnetization and to interpret properly experiments on the scattering and absorption of polarized neutrons by polarized nuclei. In particular, the sign of  $A$  must be known in order for the angular momentum of the levels of a compound nucleus to be determined. The purpose of this investigation is to account for the form of

(2) Zavoisky, E., "Paramagnetic Relaxation of Liquid Solutions for Perpendicular Fields," *J. Phys. USSR* 9, 211 (1945).

(3) Rose, M. E., "Polarization of Nuclear Spins," OPNL-48 (June 9, 1948).

(4) Gorter, C. J., "A New Suggestion for Aligning Certain Atomic Nuclei," *Physica* 14, 504 (1948).

(5) Bleaney, B., "Nuclear Specific Heats in Paramagnetic Salts," *Phys. Rev.* 78, 214 (1950).

the hfs interaction and to determine the sign of  $A$  by use of theoretical considerations.

The ground state of  $Mn^{++}$  is a  $(3s)^2 (3d)^5 {}^6S$  state which gives no hfs at all. Abragam<sup>(6)</sup> has suggested that the observed effect may be due to admixture of an excited state,  $(3s)^1 (3d)^5 (4s)^1 {}^6S$  which has unpaired  $s$  electrons. We can show that this configuration, with the two  $s$  electrons in a  ${}^3S$  state, is excited by the intraatomic spin-dependent forces due to the requirements of the Pauli principle. Specifically, the added exchange term in the Hartree-Fock equations can be regarded as a perturbation upon a zero-order Hamiltonian which is the ordinary Hartree equation. This perturbation takes the form

$$H' = J_{ik}(r, r') \vec{S} \cdot \vec{s} \quad (2)$$

where  $\vec{S}$  is the spin ( $5/2$ ) of the unpaired  $3d$  electrons,  $\vec{s}$  is the spin of a given  $3s$  electron, and  $J_{ik}$  is an operator depending on the wave functions of the  $3d$  and  $3s$  electrons. Using this interaction, the admixture of the excited state is given by

$$\begin{aligned} (4s | J_{ik} | 3s) = & \int_0^\infty R_{4s}(r') R_{3d}(r') \left[ \frac{1}{r'^3} \int_0^{r'} R_{3d}(r) R_{3s}(r) r^4 dr + \right. \\ & \left. + r'^2 \int_{r'}^\infty \frac{R_{3d}(r) R_{3s}(r)}{r} \right] r'^2 dr' \quad (3) \end{aligned}$$

and the form of the interaction is given by (1). The Pauli principle also introduces a spin-independent force, but this results in a  ${}^1S$  state for the two electrons with no resultant hfs.

To determine the sign of  $A$  the proper Hartree-Fock radial functions for both the normal and excited configurations must be used. Unfortunately, the

(6) Abragam, A., "Paramagnetic Resonance and Hyperfine Structure in the Iron Transition Group," *Phys. Rev.* 79, 534 (1950).

only functions available are the Hartree solutions of the normal iron atom. Computation of Eq. (3) by using these functions gave the result

$$A = + 0.0017 \text{ cm}^{-1}$$

Unpublished results by Bleaney indicate that  $A$  has a negative sign. Since the overlap integrals are very sensitive to the choice of the proper wave functions, proper comparison of these results should be made only after the Hartree-Fock wave functions are available for  $\text{Mn}^{++}$ .

**On the Energy-Loss Mechanism of Slow Ions (S. Tamor).** The trajectory of an ion passing through a stopping material is conveniently divided into three regions. When the ion velocity  $v$  is small compared with the orbital-electron velocities, the energy loss is due predominantly to elastic collisions. For  $v$  of the order of orbital velocities, electron capture and loss are the important effects, while for still higher velocities it is the ionization loss.

The calculation of the elastic scattering cross-sections, as described in the previous quarterly report (ORNL-940, p. 52) is now well underway. For ion velocities greater than about  $4 \times 10^8$  cm/sec (proton energy of about 80 Kev) and for sufficiently heavy atoms, the energy loss can be treated classically with the aid of the Fermi-Thomas model. The stopping power may be written

$$-\frac{dE}{dx} = \frac{4\pi N Z e^4}{m v^2} B$$

where the stopping number  $B$  is given by

$$B = \log 2mv^2 \int_0^{2mv^2} N(E) dE - \int_0^{2mv^2} \log E N(E) dE$$

$N(E)$  is here the number of electrons of binding energy between  $E$  and  $E + dE$  and is equal to

$$\frac{3}{2} \frac{\mu}{e^2} \int_0^{x_{\max}} x^2 \sqrt{\frac{\phi(x)}{x} - \frac{\mu E}{Ze^2}} dx$$

where  $\phi(x)$  is the Fermi-Thomas function,  $\mu$  is a unit of length equal to  $0.885 a_0/Z^{1/3}$ , and  $x_{\max}$  is the root of the integrand.

The region of intermediate velocities is more difficult to treat, and there is at present no satisfactory theory of the energy loss of such ions. An attempt is now being made to formulate some sort of semiempirical theory of the capture and loss process with the aim in view of determining the relative importance of the electronic and nuclear (elastic) collisions.

**Neutron-Deuteron Scattering** (F. G. Prohammer and T. A. Welton). An attempt is being made to use the available information on the  $H^3$  binding energy and the low-energy neutron-deuteron scattering to obtain valid new information on the nuclear forces. It is known that  $H^3$  has a single bound state. This is apparently a nearly pure  ${}^2S_{1/2}$  state, requiring about 6 Mev of energy to dissociate it into a deuteron plus a neutron. If slow neutrons are scattered by deuterons, an epithermal scattering cross-section  $\sigma_s$ , as well as a coherent cross-section  $\sigma_c$ , can be observed:

$$\sigma_s = 4\pi \left[ \frac{2}{3} a_4^2 + \frac{1}{3} a_2^2 \right] \tag{1}$$

$$\sigma_c = 4\pi \left[ \frac{2}{3} f_4 + \frac{1}{3} f_2 \right]^2$$

The quantities  $a_2$  and  $a_4$  are the scattering lengths for the  ${}^2S_{1/2}$  and  ${}^4S_{3/2}$  states, respectively. The quantities  $f_2$  and  $f_4$  are the corresponding amplitudes for scattering of neutrons by bound deuterons [ $f = (3/2)a$ ].

It is known that  $\sigma_s = 3.3$  barns. Shull and Wollan<sup>(7)</sup> have determined a value for  $\sigma_c$  of  $5.2 \pm 0.4$  barns by diffraction of neutrons from sodium

(7) Shull, C. G., and Wollan, E. O., "Coherent Scattering Amplitudes as Determined by Neutron Diffraction," *Phys. Rev.* 81, 527 (1951).

deuteride. Recent measurements by Hurst and Alcock<sup>(8)</sup> at Chalk River on the scattering of thermal neutrons from deuterium gas yield a value  $\sigma_c = 5.8 \pm 0.2$  barns. A reasonable value seems to be  $\sigma_c = 5.5$  barns. In addition, it is known that the sign of the coherent amplitude  $[(2/3)f_4 + (1/3)f_2]$  is positive (same sign as for the triplet  $n,p$  scattering).

The above information yields two simultaneous equations for  $a_2$  and  $a_4$ . Unfortunately, one is linear and one is quadratic, so that two sets of roots result. These are:

$$a_2 = 8.1 \times 10^{-13} \text{ cm} \quad a_4 = 2.6 \times 10^{-13} \text{ cm} \quad (\text{A})$$

and

$$a_2 = 0.8 \times 10^{-13} \text{ cm}, \quad a_4 = 6.2 \times 10^{-13} \text{ cm} \quad (\text{B})$$

In order to decide between these possibilities, use can be made of the further information that a single bound  ${}^2S_{1/2}$  state lies 6 Mev beneath the energy of the scattering problem, and that there is no bound  ${}^4S_{3/2}$  state.

Write

$$k \cot \delta_2 = -\frac{1}{a_2} + b_2 k^2 + 0(k^4) \quad (2)$$

$$k \cot \delta_4 = -\frac{1}{a_4} + b_4 k^2 + 0(k^4)$$

where  $k$  is the (relative) neutron wave number,  $\delta_2$  and  $\delta_4$  are the doublet and quartet phase shifts,  $a_2$  and  $a_4$  are the scattering lengths, and  $b_2$  and  $b_4$  are lengths (effective ranges) of the order of magnitude of  $10^{-13}$  cm (for simplicity take  $b_2 = b_4 = b = 10^{-13}$  cm and neglect terms in  $k^4$ ). If Eq. (2) is analytically continued for imaginary  $k$  ( $k = -iK$ , with  $K$  positive), a bound

(8) Hurst, D. G., and Alcock, N. Z., "The Scattering Lengths of the Deuteron," *Phys. Rev.* 80, 117 (1950).

state will be found at a zero of  $e^{i\delta}$  (vanishing scattering matrix). This can be seen by considering the analytic continuation of the neutron wave function

$$\sin(kr + \delta) = \frac{e^{i\delta}e^{ikr} - e^{-i\delta}e^{-ikr}}{2i} \longrightarrow \frac{e^{i\delta}e^{Kr} - e^{-i\delta}e^{-Kr}}{2i} \quad (3)$$

Here  $e^{i\delta}$  appears as the coefficient of the unwanted (for a well-behaved bound-state wave function) term which becomes exponentially large as  $r \rightarrow \infty$ . If  $e^{i\delta}$  is set equal to zero, Eqs. (2) become:

$$-K_2 = -\frac{1}{a_2} - bK_2^2 \quad (4)$$

$$-K_4 = -\frac{1}{a_4} - bK_4^2$$

where  $K_2$  and  $K_4$  (if a root can be found) are related to the doublet and quartet binding energies by

$$\frac{2}{3}|E_2| = \frac{\hbar^2 K_2^2}{2M} \quad (5)$$

$$\frac{2}{3}|E_4| = \frac{\hbar^2 K_4^2}{2M}$$

where  $M$  is the neutron mass.

From Eqs. (4),

$$K_2 = \frac{1 - \sqrt{1 - 4b/a_2}}{2b} \quad (6)$$

$$K_4 = \frac{1 - \sqrt{1 - 4b/a_4}}{2b}$$

where the sign of the square root has been so chosen as to make  $K = 1/a$  as  $b \rightarrow 0$ .

The pair of roots (A) yields

$$K_2 = 0.5 \times 10^{13} \text{ cm}^{-1}, \quad K_4 = \text{a complex number} \quad (\text{A})$$

while the set (B) yields

$$K_4 = 0.20 \times 10^{13} \text{ cm}^{-1}, \quad K_2 = \text{a complex number} \quad (\text{B})$$

It then appears that the set (A) agrees qualitatively with the criterion which has been set up, while the set (B) definitely does not. The  $K_2$  from Eq. (A) gives a doublet binding energy of only about 1 Mev, so that the quantitative agreement with the experimental value is disappointing. It is likely that the presence of the threshold for deuteron disintegration only 2.2 Mev above zero energy so distorts the energy dependence of  $k \cot \delta$  that terms in  $k^4$  are needed to give a good value for the binding energy.

It then seems almost certain that the solution (A) is actually correct, so that

$$a_2 = 8.1 \times 10^{-13} \text{ cm} \quad \text{and} \quad a_4 = 2.6 \times 10^{-13} \text{ cm} \quad (7)$$

The quartet scattering length should contain very good information as to the strength of the triplet neutron-neutron interaction, and a good calculation is being performed. It is unfortunate that examination of existing calculations in the light of the detailed information in Eq. (7) strongly indicates that the usual approximations are not valid.

**Theory of Scattering and Capture of Slow Neutrons (T. A. Welton).** A simple derivation has been attempted of the usual Breit-Wigner one-level formula. Consider first the case of pure neutron scattering, without capture, and for simplicity neglect the spins of the neutron and target nucleus. The scattering is then completely described (for slow neutrons) by a phase shift for the S neutron wave  $\delta$ . Define

$$\phi(k) = k \cot \delta \quad (1)$$

A derivation from first principles is given of the formula

$$\frac{d\phi}{d(k^2)} = -b(k) \equiv - \frac{\int d\tau_N \int d\tau (\psi^2 - \psi_\infty^2)}{\int d\tau_N u^2} \quad (2)$$

Here  $\int d\tau_N$  is an integration over the configuration space of the target nucleus, while  $\int d\tau$  is an integration over the space of the incident neutron. The function  $u$  is the (real) wave function for the ground state of the target nucleus. The function  $\psi$  is the (real) wave function for the compound nucleus, and  $\psi_\infty$  is equal to  $\psi$  in that portion of the total configuration space for which the incident nucleus is outside the target nucleus (external region). Write  $\psi_\infty$  everywhere as

$$\begin{aligned} \psi_\infty &= \frac{\sin(kr + \delta)}{r \sin \delta} u \\ &= \left[ \frac{\cos kr}{r} + k \cot \delta \frac{\sin kr}{kr} \right] u = \left[ \frac{\cos kr}{r} + \phi \frac{\sin kr}{kr} \right] u \\ &\approx \left[ \frac{1}{r} + \phi \right] u \text{ for } kr \ll 1 \end{aligned} \quad (3)$$

At the nuclear boundary ( $r = R$ ),  $\psi_\infty$  (and hence  $\psi$ ) is equal to

$$(1/R)(1 + R\phi)u$$

It seems reasonable to assume that the shape of  $\psi^2$  is essentially independent of energy, but that its size is proportional to the factor  $(1 + R\phi)^2$  which determines the energy variation of its value at the boundary of the external

region. Equation (2) then becomes

$$\frac{d\phi}{d(k^2)} = -(1 + R\phi)^2 b_0 \quad (4)$$

where  $b_0$  is the value taken on by  $b(k)$  for  $k = k_0$  (the resonant energy). Note that a resonance is defined as a zero of  $\phi$ . Equation (4) is easily integrated:

$$\phi = -\frac{1}{R} + \frac{1/R}{1 + b_0 R(k^2 - k_0^2)} \quad (5)$$

The scattering cross-section is given by

$$\sigma_s = \frac{4\pi}{k^2} \sin^2 \delta = \frac{4\pi}{k^2 + \phi^2} \quad (6)$$

$$\sigma_s = 4\pi \left| \frac{1}{\phi + ik} \right|^2$$

Substitution of Eq. (5) in Eq. (6) leads to

$$\sigma_s = \frac{4\pi}{k^2} \left| \frac{\frac{\Gamma_n}{2}}{-(E - E_0) + \frac{i\Gamma_n}{2}} - kR \right|^2 \quad (7)$$

with

$$\Gamma_n = \frac{\hbar^2 k}{Mb_0}$$

This is the usual Breit-Wigner scattering formula, with  $\Gamma_n$  defined in terms of the quantity  $b_0$ . Note that  $b_0$  is independent of energy, and hence  $\Gamma_n$  is proportional to  $k$ . The quantity  $-kR$  is simply the low-energy approximation to  $e^{-ikR} \sin(-kR)$ , which is the potential scattering amplitude multiplied by  $k$ .

It is further shown that a simple definition can be made for  $T$ , the time spent by the incident neutron inside the target nucleus:

$$\begin{aligned}
 T &= \frac{2M}{\hbar k} \frac{d}{dk} (\delta + kR) \\
 &= \frac{2}{v} R + \frac{d\delta}{dk}
 \end{aligned}
 \tag{8}$$

where  $v$  is the (group) velocity of the incident neutron. Equation (8) can be made plausible by consideration of two special cases: (1) If the nucleus does not affect the neutron in any way, then  $\delta = 0$  and  $T = 2R/v$ , which is just the time required for the free neutron to traverse the diameter of the "nucleus"; (2) if, on the other hand, the nucleus scatters as a hard sphere,  $\delta = -kR$  and  $T = 0$ , which is reasonable since the neutron cannot enter a hard sphere. It is also of interest to note that at a resonance  $\phi = 0$ ,  $T = 4\hbar/\Gamma_n$  very nearly, which is just four times the mean life of the compound nucleus against neutron emission.

Next define a quantity  $\pi/k^2$ , which is the cross-section for incidence on the nucleus, and a quantity  $\Gamma_a/\hbar$ , which is the probability per unit time that the assembled compound nucleus decays by an absorption process (radiation, fission, etc.) rather than by neutron emission. In terms of these quantities the absorption cross-section is easily written as

$$\sigma_a = \frac{\pi}{k^2} \frac{\Gamma_a}{\hbar} T
 \tag{9}$$

This equation holds only under the assumption of weak absorption ( $\Gamma_a \ll \Gamma_n$ ); its extension to the case of strong absorption appears simple, but has not yet been made.

Equation (9) leads to the value of  $\sigma_a$  at resonance which follows from the Breit-Wigner formula (with weak absorption). It also leads to the same shape near resonance. Discrepancies appear for energies off resonance by more than the half-width. These differences are being analyzed, and it is hoped that available experiments can be used to decide between the various possibilities.

**A Note on Isotropy of Nuclear Gamma Radiation** (G. B. Arfken, L. C. Biedenharn, and M. E. Rose). In ORNL-865 it was conjectured that if one has isotropic  $2^L$  pole gamma radiation from a level  $j$  and  $L \geq j - \frac{1}{2}$ , then all gamma radiation from that state must be isotropic. The condition  $L \geq j - \frac{1}{2}$  was shown necessary. It is now possible to show that it is also sufficient for cases of physical interest. The angular distribution function may be written

$$\begin{aligned}
 W(\theta) &= \sum_{n,M} a_n (C_{nM}^{jLJ})^2 F_L^M(\theta) \\
 &\equiv \sum_n a_n F_{LjJ}^n(\theta)
 \end{aligned}$$

where  $a_n$  gives the level population,  $C_{nM}^{jLJ}$  is a Clebsch-Gordon coefficient, and  $F_L^M$  is the usual distribution function. Using the familiar properties of the rotation group  $F$  may be expressed in terms of spherical harmonics and Racah functions. Dropping common factors,

$$F_{LjJ}^n = \sum_{i=0}^L C_{n-n}^{jj2i} C_{l-l}^{LL2i} W(L, 2i, J, j; L, j) Y_{2i}^0(\cos \theta)$$

It may be seen that the  $F_{LjJ}^n$  are linearly independent for  $L \geq j - \frac{1}{2}$  unless  $C_{l-l}^{LL2i}$  or the Racah function,  $W$ , vanishes for some  $i$ ,  $0 \leq i \leq L$ . It has been

found that  $C_{l-1}^{LL^2i}$  does vanish for  $(L, i) = (14, 10)$ ,  $(492, 348)$ , and  $(16730, 11830)$ , and, in fact, there is an infinite number of larger solutions. Mr. Coveyou of the Mathematics Panel has verified these solutions and shown that no smaller ones ( $L > 0$ ) exist. Since  $2^{14}$ ,  $2^{492}$ , and  $2^{16730}$  pole radiations are rather highly forbidden, these exceptions are considered amusing rather than serious. This analysis may also be applied to show that the  $F_L^M$  for fixed  $L$  form a linearly independent set except for  $L = 14, 492, 16730$ , and certain larger  $L$ . While the properties of  $W$  are known only imperfectly, it can be shown that for the case of interest,  $B^{11}(p, \gamma)C^{12}$  where  $J = 0$ ,  $W = (2j + 1)^{-1}$ , and therefore does not vanish. Hence for  $J = 0$  and, so far as is now known, for all other cases of physical interest, the condition  $L \geq j - \frac{1}{2}$  is sufficient as well as necessary. A detailed analysis will be published in connection with the forthcoming report on angular correlation of three successive radiations.

**Symmetry Between Positron and Negatron Spectra in Beta Decay** (L. C. Biedenharn and M. E. Rose). This investigation, of which a preliminary report was given in the last quarterly report (ORNL-940), has now been completed. Our final conclusion is that the assumption of symmetry between positron and negatron spectra in beta decay in the limit of zero nuclear charge (other factors, such as nuclear matrix elements, being the same) places the limitation that only the  $(S, A, P)$  and/or  $(V, T)$  covariants may be mixed. This conclusion was originally reached by De Groot and Tolhoek<sup>(9)</sup> and, despite all previous statements to the contrary (ORNL-940), we now confirm this result.

(9) De Groot, S. R., and Tolhoek, H. A., "On the Theory of Beta Radioactivity. I. The Use of Linear Combinations of Invariants in the Interaction Hamiltonian," *Physica* 16, 456 (1950).

